INVESTIGATION OF ENANTIOSELECTIVE ASYMMETRIC CATALYSIS IN MICHAEL-ADDITION TYPE REACTIONS USING WERNER SALTS AND THEIR ANION INVOLVEMENT

A Thesis

by

BAILEY LAUREN JAMESON

Submitted to the Graduate and Professional School of
Texas A&M University
in partial fulfillment of the requirements for the degree of

MASTER OF SCIENCE

Chair of Committee,	John A. Gladysz
Committee Members,	David Powers
	Stephen Talcott
Head of Department,	Simon W. North

August 2022

Major Subject: Chemistry

ABSTRACT

Enantioselective additions of malonate esters to nitroalkenes can be catalyzed by a variety of salts of chiral cobalt(III) trications $[Co(1,2\text{-diamine})_3]^{3+}$ in the presence of nitrogen donor bases in acetone. Catalysts that feature enantiopure 1,2-diphenylethylenediamine are particularly effective, and the base can also be incorporated into one of the counter anions, for example a (substituted) nicotinate. This study shows that such additions can be carried out under solvent free conditions and with reduced reaction times using ball milling, further enhancing the "green" credentials of this large family of earth-abundant-metal catalysts. The effect of various reaction variables are probed (base, counter anions, loading, time, quantity of balls, etc.), and the optimized conditions applied to twelve nitroalkenes, affording products in average yields and ee values of 89% and 74%. The enantioselectivities appear slightly lower than for analogous reactions in solution (0 °C), and possible factors and remedies are discussed. These tricationic Co(III) species were also analyzed using Electrospray Ionization-Mass Spectrometry to determine if the anions “fly” with the cation for further mechanistic analysis. Only half showed anions “flying” with the cation: Λ-(*S*,*S*)-**2**$^{3+}$ 2Cl$^-$, Λ/Δ-(*S*,*S*)-**2**$^{3+}$ 2Cl$^-$BAr$_f^-$, Λ-(*S*,*S*)-**2**$^{3+}$ Cl$^-$BAr$_f^-$Nic$^-$, and Λ-(*S*,*S*)-**2**$^{3+}$ 3BF$_4^-$. While anionic impurities were found in several cases, the larger, bulkier anions seemed to become ionized themselves leaving no indication of intact cation-anion species post-ionization. Enhanced purification techniques are shown to improve the removal of unwanted anions.

DEDICATION

My Fiancé, Friends, and Family.

ACKNOWLEDGEMENTS

The authors thank the Welch Foundation (Grant A-1656) for support, Prof. David Powers and his research group for access to their ball mill, and Mr. Tim Renningholtz for helpful discussions.

CONTRIBUTORS AND FUNDING SOURCES

Contributors

Part 1. Faculty Committee Recognition

This work was supervised by a dissertation committee consisting of Dr. John A. Gladysz and Dr. David Powers of the Department of Chemistry, and Dr. Stephen Talcott of the Department of Nutrition.

Part 2. Student/Collaboration Contributions

The work in Chapter 1 was completed by the student in collaboration with Connor Q. Kabes of the Department of Chemistry, who contributed equally to this project.

The work in Chapter 2 was completed by the student in collaboration with Dr. Yohannes Rezenom and thus the use of TAMU/LBMS and Dr. Yohannes Rezenom are acknowledged.

All crystal structures were determined by crystallographers Dr. Kevin Gagnon of the Advanced Light Source, Lawrence Berkeley National Laboratory, 6 Cyclotron Road, Berkeley, CA 94720, and Nattamai Bhuvanesh of the Department of Chemistry.

All other work conducted for the dissertation was completed by the student independently.

Part 3. Funding

This work was made possible in part by the Welch Foundation under Grant Number A-1656.

TABLE OF CONTENTS

Page

LIST OF FIGURES

LIST OF CHARTS

Page

LIST OF TABLES

1 INTRODUCTION

1.1 Introduction

Alfred Werner was an advantageous chemist in the early 20th century, specifically between 1911 and 1912. In just two years, he published five articles discussing his various discoveries on coordination chemistry.[1] One of which was the chiral resolution of $[Co(en)_3]^{3+}$ ($\mathbf{1}^{3+}$, Figure 1.1) (en = ethylenediamine) into its enantiomers, introducing this trication as one of the first chiral inorganic species to be separated into its enantiopure form. Further back in 1848, Pasteur was able to separate tartrate salts into their respective diastereomers upon crystallization, hence Werner's work began with the tartrate salts of $\mathbf{1}^{3+}$. Syntheses as such continue to appear in inorganic textbooks as a classic method for enantiopurification of these salts.[2]

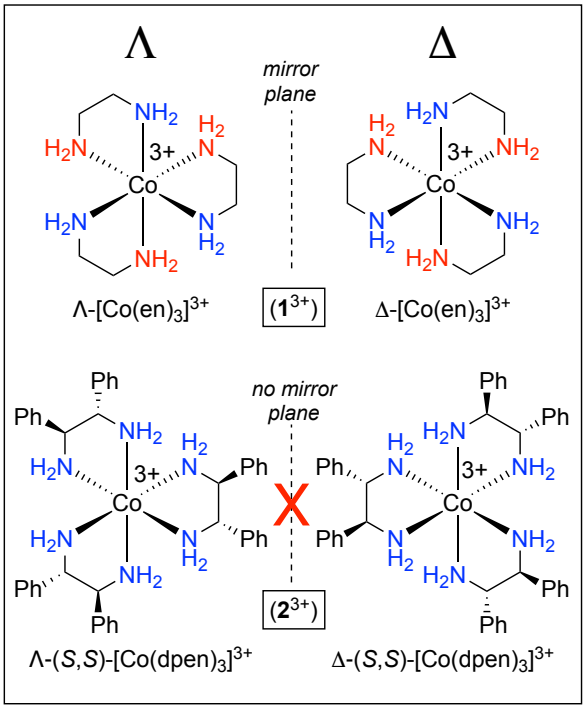

Figure 1.1. Stereoisomers of the 1,2-en Co(III) tricationic salts.

Diving into the structure of these tricationic species, the primary coordination sphere contains the metal at which en ligands are covalently bound. These complexes are considered "chiral at metal", which corresponds to its D_3 symmetry.[3] These D_3 symmetrical complexes are indicated as such due to the presence of two C_3 faces and two C_2 faces, the former with three syn-

periplanar NH groups per face and the latter with two, as seen in Figure 1.2. These protons are diastereotopic, producing one signal each for the C_3 and C_2 faces, further aligning with the properties of a chiral molecule.

Each enantiomer is often denoted in terms of Λ/Δ pertaining to the enantiomeric form in either a "left-handed" or "right-handed" fashion, respectively.[4,5] This symmetry can further be analyzed with the migration of en to the diphenylethylenediamine (dpen) derivative, $[Co(dpen)_3]^{3+}$ ($\mathbf{2}^{3+}$, Figure 1.1). This introduces the possibility for diastereomers to form: $\Lambda/(S,S)_3$ and $\Delta/(S,S)_3$ alongside their enantiomers $\Lambda/(R,R)_3$ and $\Delta/(R,R)_3$.

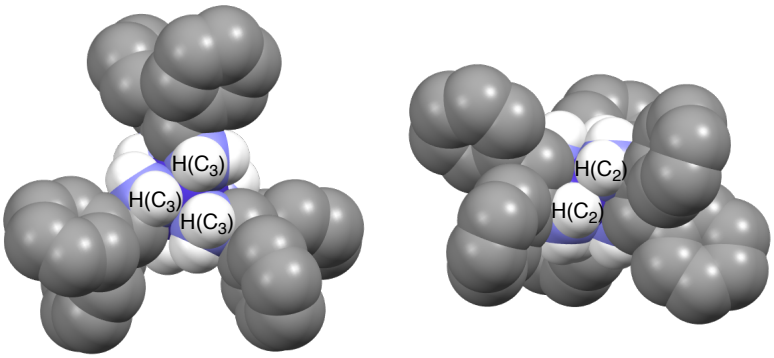

Figure 1.2. Space filling representations of crystal structures of $\mathbf{2}^{3+}$ with labelled syn-periplanar NH groups.

Within the second coordination sphere, 12 Lewis-acidic NH groups are available for hydrogen bonding to the anions in solution as well as protic solvents.[6] This indicates the possibility for these salts to act as catalysts in organic reactions by activation of Lewis-basic organic substrates via hydrogen-bonding. In this case, any species occupying a face of the trication would require dissociation prior to substrate activation for enhanced catalytic activity. It is often seen that the solvent of choice and the varying anions present affect catalytic results.[7]

1.2 Generations of Werner Catalysts

As stated previously, the synthesis and chiral resolution of the Werner tartrate salts are used in organic chemistry teaching labs at several universities due to its rudimentary synthetic pathway and low cost. When $\mathbf{1}^{3+}$ was synthesized under aqueous aerobic conditions with tartrate

salt anions, solubility in less polar solvents (i.e. toluene, hexanes, THF, chloroform) was limited.[8] Modifications of the anions alternatively incorporated pseudohalides, such as $\mathbf{1}^{3+}$ $3Cl^-$, resulting in a similar solubility profile. Additionally, the use of more lipophilic anions such as the tetrafluoroborates and tetraarylborates: tetrakis(3,5-bis(trifluoromethyl)phenyl)borate (BAr_f^-), BF_4^-, and $B(C_6F_5)_4^-$ increased the catalyst solubility in organic solvents.[9] By limiting solvent interaction with the NH groups with the aid of aprotic organic solvents, the competition for hydrogen bonding to the substrate for activation decreases. This is also seen due to the poor coordinating ability of these borates.[10]

The synthesis of these trication/anion pairings from the iodide salt $\mathbf{1}^{3+}$ $3I^-$, was described by Ganzmann in 2008.[8] The anion metathesis began with an aqueous solution of $\mathbf{1}^{3+}$ $3I^-$ (1 mol) and $NaBAr_f$ (3 mol) in CH_2Cl_2. Upon extraction of $\mathbf{1}^{3+}$ $3BAr_f^-$ into the organic layer, the product was dried to produce an analytically pure solid, $\mathbf{1}^{3+}$ $3BAr_f^-$. Seen with most Werner salts, traces of water seemed to be carried across the solvent barrier by the trication as determined by thermogravimetric analysis.[11] As these borate anions are poorly coordinating, 14 hydrates were found to travel with the cation, producing $\mathbf{1}^{3+}$ $3BAr_f^-$ • 14 H_2O. While multiple drying methods are performed on the sample, the humid Texas air consequently rehydrates the salts. The anion metathesis is depicted in Figure 1.3 below.

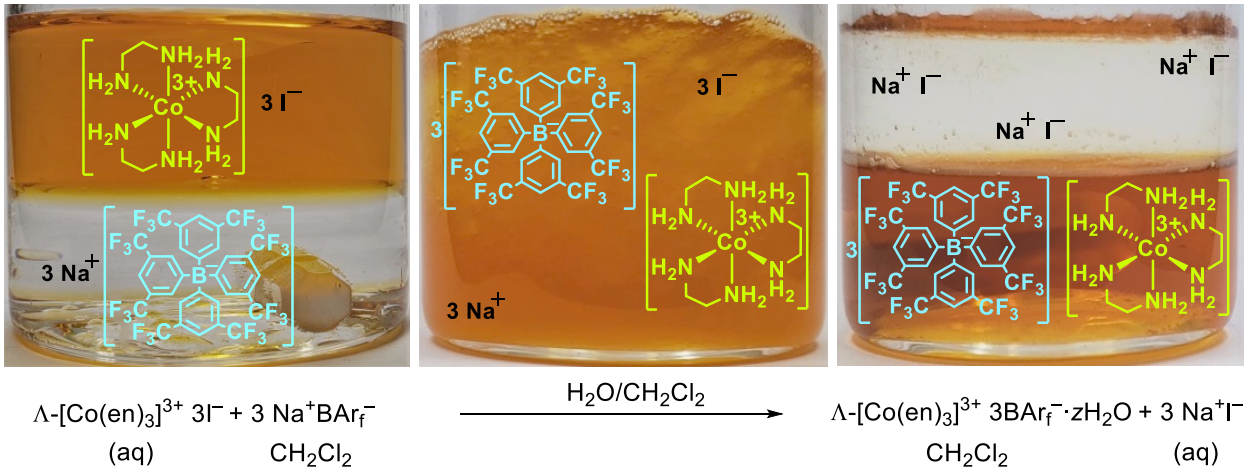

Figure 1.3. Anion metathesis of $\mathbf{1}^{3+}$ with visual changes in solubility preferences.

These first-generation salts were tested as catalysts in various reactions regarded as Michael addition reactions. Alongside the Co(III) catalyst, salts with substitutions of the metal center, Λ/Δ-$[M(en)_3]^{n+}$ $n(BAr_f^-)$ (M/n = Cr/3, Rh/3, Ir/3, Pt/4), were tested and summarized in Figure 1.4.[11]

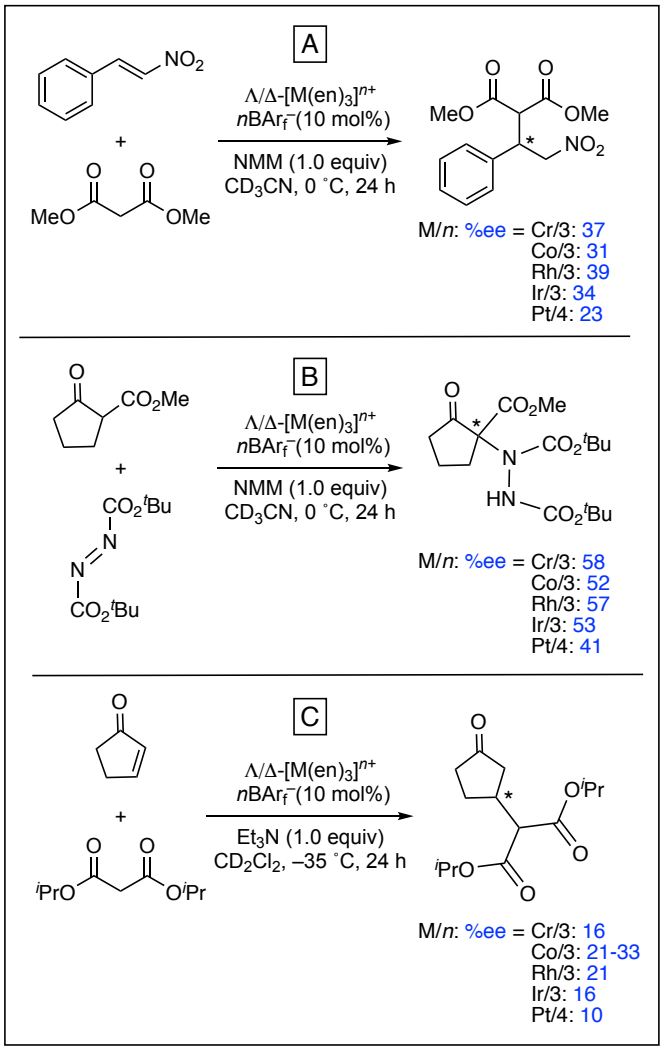

Figure 1.4. Michael addition catalytic test reactions. NMM = *N*-methylmorpholine.

Throughout each reaction enantioselectivities varied minimally between each metal, with Cr(III) and Rh(III) providing the best overall. It can be seen that the Pt(IV) complex gave the poorest results for each case, possibly due to interactions with the external base derived from the greater Brønsted acidity (pK_a 5.5) of the catalyst.[12]

Derivatives of the first-generation catalyst to incorporate aryl rings on the en backbone were established in the 1970's and utilized by the Gladysz group starting in 2008.[13,14] The source of the aryl rings starts with the commercially available, relatively cheap enantiopure dpen ligand.[15] The synthesis of $\mathbf{2}^{3+}$ $3Cl^-$ and subsequent products of anion metathesis is shown in Figure 1.5.

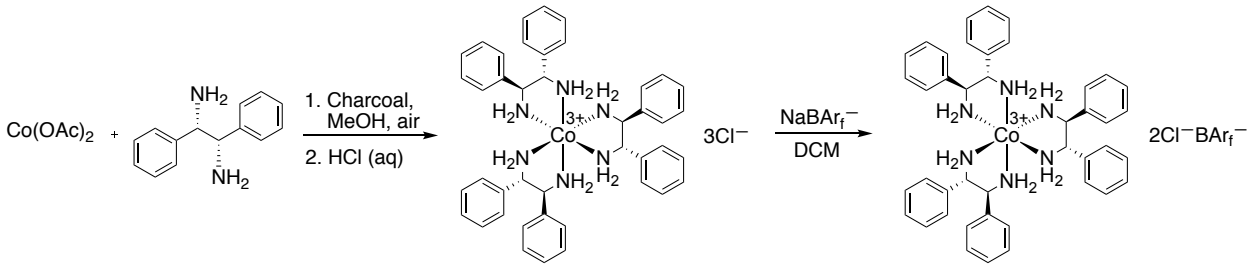

Figure 1.5. Synthesis of second-generation Werner catalysts.

The addition of charcoal acts as a redox catalyst to produce small amounts of substitution-labile Co(II), resulting in Co(III).[16] Like that of the first-generation catalysts, tetraarylborate anions were incorporated with $\mathbf{2}^{3+}$.[14] It was determined that only one BAr_f^- anion was necessary for solubility in aprotic organic solvents when the more lipophilic dpen ligand was introduced. By only including one BAr_f^- anion, cost of synthesis is reduced as well as the molecular weight of the salt. It was suggested computationally that the Λ-(*S*,*S*)-$\mathbf{2}^{3+}$ prefers counteranions that are good hydrogen-bond acceptors while the Δ- diastereomer prefers poor hydrogen-bond acceptors. This was considered to be directly related to the NH···HN distances on both C_2 and C_3 faces (2.63 Å vs 2.39 Å, respectively on the C_3 face).[14,17]

Reaction A seen in Figure 1.4 was repeated for Λ-(*S*,*S*)-$\mathbf{2}^{3+}$ $2Cl^-BAr_f^-$ as well as Λ-(*S*,*S*)-$\mathbf{2}^{3+}$ $2BF_4^-BAr_f^-$ and Λ-(*S*,*S*)-$\mathbf{2}^{3+}$ $3BF_4^-$, affording great yields and enantioselectivities (yield/ee: 94, 97, 97/ 87, 90, 93, respectively).[18] Throughout each scenario, it was determined that the cobalt stereocenter is configuration determining, thus Λ and Δ give opposite enantiomeric products. Upon investigating various other aryl derivatives of the dpen catalyst, hydroxy-substituted phenyl rings did not out-compete the Λ-(*S*,*S*)-$\mathbf{2}^{3+}$ catalyst.

The Michael addition test reactions require the addition of an external base, such as *N*-methylmorpholine (NMM), NEt_3, and pyridine (Py). The third-generation of catalysts investigates the incorporation of a nitrogenous base into the cation/anion, considering them bifunctional. This term coincides with the salt acting as both a catalyst and base in solution. Originally, the alteration of the en ligand backbone was synthesized to include a tertiary amine chain, lowering the symmetry of the salt and eliminating the need for an external base.[19] Depending on the length of the tertiary amine chain ($(CH_2)_nNMe_2$) the ligand can be synthesized in six to nine steps in a moderate yield (26%). While catalytic activity was observed with good enantioselectivities, its synthesis is lengthy. This led to the investigation of basic anions, such as nicotinate derivatives, some of which can be seen in Figure 1.6.[20] The best and most hydrogen bond accepting bifunctional catalyst was determined to be Λ-(*S*,*S*)-$\mathbf{2}^{3+}$ $2Cl^-BAr_f^-$6-NH_2-Nic^- (yield/ee: 95%/87%) in the dimethyl malonate and *trans*-β-nitrostyrene Michael addition test reaction. Not only are the catalytic results impressive, these bifunctional anion catalysts only require a two-step synthesis from the starting $Co(OAc)_2$ compound.

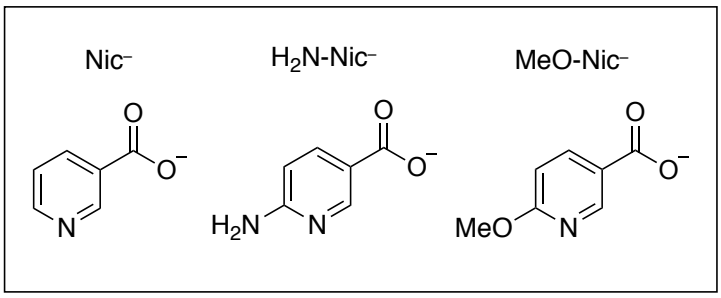

Figure 1.6. Bifunctional anions as nicotinate derivatives.

1.3 Conclusion

Since the 1900's, the Werner salts have become a competitive player in catalysis. From the first-generation catalyst $\mathbf{1}^{3+}$ to the second-generation $\mathbf{2}^{3+}$, enhanced yields and enantioselectivities are observed (yield/ee: >94%/ >87%). With the incorporation of tetrafluoroborate and tetraarylborate anions, specifically BAr_f^-, new solubility profiles allow catalysis in aprotic organic solvents. By incorporating basic entities into the salts by either tertiary amine chains on the en ligand or nicotinate derivatives as anions, the necessity for external bases is removed and yields

and enantioselectivities are consistently high (yield/%ee: up to 95%/87%). Optimizations of catalytic activity continues to be investigated for these Werner catalysts.

1.4 References. (All titles are given in the capitalization format of the original article)

(1) (a) Werner, A. Zur Kenntnis des asymmetrischen Kobaltatoms. I. *Ber. Dtsch. Chem. Ges.* **1911**, *44*, 1887–1898. (b) Werner, A. Zur Kenntnis des asymmetrischen Kobaltatoms. II. *Ber. Dtsch. Chem. Ges.* **1911**, *44*, 2445–2455. (c) Werner, A. Zur Kenntnis des asymmetrischen Kobaltatoms. III. *Ber. Dtsch. Chem. Ges.* **1911**, *44*, 3272–3278. (d) Werner, A. Zur Kenntnis des asymmetrischen Kobaltatoms. IV. *Ber. Dtsch. Chem. Ges.* **1911**, *44*, 3279–3284. (e) Werner, A. Zur Kenntnis des asymmetrischen Kobaltatoms. V. *Ber. Dtsch. Chem. Ges.* **1912**, *45*, 121–130.

(2) Girolami, G. S.; Rauchfuss, T. B.; Angelici, R. J. Synthesis and Technique in Inorganic Chemistry: A Laboratory Manual, 3rd ed.; University Science Books: Sausalito, CA, 1999; pp 143–151.

(3) (a) Brunner, H. Optically Active Organometallic Compounds of Transition Elements with Chiral Metal Atoms. *Angew. Chem., Int. Ed.* **1999**, *38*, 1194–1208. (b) Fontecave, M.; Hamelin, O.; Menage, S. *Top. Organomet. Chem.* **2005**, *15*, 271–288. (c) Constable, E. C. Stereogenic metal centers – from Werner to supramolecular chemistry. *Chem. Soc. Rev.* **2013**, *42*, 1637–1651. (d) Zhang, L.; Meggers, E. Stereogenic-Only-at-Metal Asymmetric Catalysts. *Chem.-Asian J.* **2017**, *12*, 2335–2342.

(4) Piper, T. S. Partial Chromatographic Resolution, Rotary Dispersion, and Absolute Configuration of Octahedral Complexes Containing Three Identical Bidentate Ligands. *J. Am. Chem. Soc.* **1961**, *83*, 3908–3909.

(5) Ehnbom, A.; Ghosh, S. K.; Lewis, K. G.; Gladysz, J. A. Octahedral Werner complexes with substituted ethylenediamine ligands: a stereochemical primer for a historic series of compounds now emerging as a modern family of catalysts. *Chem. Soc. Rev.* **2016**, *45*, 6799–6811.

(6) Ghosh, S. K.; Ehnbom, A.; Lewis, K. G.; Gladysz, J. A. Hydrogen bonding motifs in structurally characterized salts of the tris(ethylenediamine) cobalt trication, $[Co(en)_3]^{3+}$; An interpretive review, including implications for catalysis. *Coord. Chem. Rev.* **2017**, *350*, 30–48.

(7) (a) Gladysz, J. A.; Boone, B. J. Chiral Recognition in π Complexes of Alkenes, Aldehydes, and Ketones with Transition Metal Lewis Acids; Development of a General Model for Enantioface Binding Selectivities. *Angew. Chem., Int. Ed. Engl.* **1997**, *36*, 550–583. (b) Kromm, K.; Zwick, B. D.; Meyer, O.; Hampel, F.; Gladysz, J. A. A New Family of Chelating Diphosphines with a Transition Metal Stereocenter in the Backbone: Novel Applications of "Chiral-at-Rhenium" Complexes in Rhodium-Catalyzed Enantioselective Alkene Hydrogenations. *Chem.- Eur. J.* **2001**, *7*, 2015–2027. (c) Delacroix, O.; Gladysz, J. A. Transition-Metal-Containing Chiral Bidentate Ligands for Enantioselective Catalysis: Non-Metallocene Architectural Units Come of Age. *Chem. Commun.* **2003**, 665–675.

(8) Ganzmann, C.; Gladysz, J. A. Phase Transfer of Enantiopure Werner Cations into Organic Solvents; An Overlooked Family of Chiral Hydrogen Bond Donors for Enantioselective Catalysis. *Chem.- Eur. J.* **2008**, *14*, 5397–5400.

(9) Riddlestone, I. M.; Kraft, A.; Schaefer, J.; Krossing, I. Taming the Cationic Beast: Novel Developments in the Synthesis and Application of Weakly Coordinating Anions. *Angew. Chem., Int. Ed.* **2018**, *57*, 13982–14024 and earlier reviews cited therein.

(10) Wititsuwannakul, T.; Hall, M. B.; Gladysz, J. A. A Computational Study of Hydrogen Bonding Motifs in Halide, Tetrafluoroborate, Hexafluorophosphate, and Tetraarylborate Salts of Cationic Ruthenium and Cobalt Guanidinobenzimidazole Hydrogen Bond Donor Catalysts; Acceptor Properties of the "BAr_f" Anion. *Polyhedron* **2020**, *187*, 114618.

(11) Maximuck, W. J.; Ganzmann, C.; Alvi, S.; Hooda, K. R.; Gladysz, J. A. Rendering classical hydrophilic enantiopure Werner salts $[M(en)_3]^{n+}$ nX^- lipophilic (M/n = Cr/3, Co/3, Rh/3, Ir/3, Pt/4); new chiral hydrogen bond donor catalysts and enantioselectivities as a function of metal and charge. *Dalton Trans.* **2020**, *49*, 3680–3691.

(12) Palmer, J. W.; Basolo, F. Effect of Transition Metal Ion on Rates of Hydrogen Exchange in Metal Ammines. *J. Inorg. Nucl. Chem.* **1960**, *15*, 279–286.

(13) (a) Bosnich, B.; Harrowfield, J. MacB. A Regional Rule for the Optical Activity of Conformational Isomers of Octahedral Transition Metal Complexes. *J. Am. Chem. Soc.* **1972**, *94*,

3425–3437. (b) Kuroda, R.; Mason, S. F. Crystal Structure and Absolute Configuration of (+)-Tris[(–)-1,2-diphenylethylenediamine]-cobalt(III) Nitrate Monohydrate. *J. Chem. Soc., Dalton Trans*. **1977**, *10*, 1016–1020.

(14) Ghosh, S. K.; Lewis, K. G.; Kumar, A.; Gladysz, J. A. Syntheses of Families of Enantiopure and Diastereopure Cobalt Catalysts Derived from Trications of the Formula $[Co(NH_2CHArCHArNH_2)_3]^{3+}$. *Inorg. Chem*. **2017**, *56*, 2304–2320.

(15) As of the submission date of this thesis, the best prices are (*R*,*R*)-dpen, $275/100 g and (*S*,*S*)-dpen, $271/100 g (https:// www.ambeed.com, accessed 29 May 2022).

(16) (a) Douglas, B. D. Racemization of Tris-(ethylenediamine)cobalt(III) Ion in the Presence of Decolorizing Carbon. *J. Am. Chem. Soc*. **1954**, *76*, 1020–1021. (b) For fascinating remarks regarding differences between types of charcoals and their catalyst lifetimes, consult the last paragraph of the experimental section of Harnung, S. E.; Kallesøe, S.; Sargeson, A. M.; Schaffer, C. E. *Acta Chem. Scand*. **1974**, *28a*, 385–398.

(17) Luu, Q. H.; Lewis, K. G.; Banerjee, A.; Bhuvanesh, N.; Gladysz, J. A. The Robust, Readily Available Cobalt(III) Trication $[Co(NH_2CHPhCHPhNH_2)_3]^{3+}$ is a Progenitor of Broadly Applicable Chirality and Prochirality Sensing Agents. *Chem. Sci*. **2018**, *9*, 5087–5099.

(18) Lewis, K. G.; Ghosh, S. K.; Bhuvanesh, N.; Gladysz, J. A. Cobalt(III) Werner Complexes with 1,2-Diphenylethylenediamine Ligands: Readily Available, Inexpensive, and Modular Chiral Hydrogen Bond Donor Catalysts for Enantioselective Organic Synthesis. *ACS Cent. Sci*. **2015**, *1*, 50–56.

(19) Ghosh, S. K.; Ganzmann, C.; Bhuvanesh, N.; Gladysz, J. A. Werner Complexes with ω-Dimethylaminoalkyl Substituted Ethylenediamine Ligands: Bifunctional Hydrogen-Bond-Donor Catalysts for Highly Enantioselective Michael Additions. *Angew. Chem., Int. Ed*. **2016**, *55*, 4356–4360.; Ghosh, S. K.; Ganzmann, C.; Bhuvanesh N.; Gladysz, J. A. Werner-Komplexe mit ω-Dimethylaminoalkyl-substitutierten Ethylendiaminliganden: bifunktionale H-Brückendonor-Katalysatoren für hoch enantioselektive Michael-Additionen. *Angew. Chem*. **2016**, *128*, 4429–4433.

(20) Kabes, Connor Q.; Lucas, Reagan F.; Gunn, Jack H.; Gladysz, John A. Chiral Cobalt(III) Tris(1,2-diamine) Catalysts That Incorporate Nitrogenous Base Containing Anions for the Bifunctional Activation of Nucleophiles and Electrophiles in Enantioselective Addition Reactions. *ACS Catal*. **2021**, *11*, 7762–7771.

2 ENANTIOSELECTIVE CATALYSIS: MICHAEL ADDITION[†]

2.1 Introduction

Over the last several decades there have been steadily increasing efforts to reduce or eliminate the use of solvents in synthesis.[1] Among the many strategies, mechanochemistry[2,3] – most commonly known as ball milling[4] – has received particular attention. This family of techniques can be readily applied to reactions involving solids. Indeed, a recent editorial in a leading green chemistry journal affirmed "Manuscripts that either minimize or totally avoid the use of solvents in catalysis are welcomed. An emerging area of interest is catalysis via mechanochemistry...".[5,6]

Accordingly, several investigators have successfully carried out enantioselective carbon-carbon and carbon-heteroatom bond forming reactions under mechanochemical conditions.[7] These have involved both metal-containing and non-metal-containing catalysts. Among the former, there has been particular interest in transitioning to earth abundant metals[8] with readily available ligand sets that do not require further additives, components, or the Shakespearean "eye of newt".[9]

For the last fifteen years, we have been developing cobalt(III) catalysts derived from the chiral trication $[Co(en)_3]^{3+}$ ($\mathbf{1}^{3+}$) depicted in Figure 2.1,[10,11] water soluble halide salts of which Werner resolved into enantiomers (termed Δ and Λ) 110 years ago.[12,13] These substitution inert species serve as hydrogen bond donors, with the coordinated NH groups providing the locus of reactivity.[10] One or more lipophilic anions, such as $B(3,5\text{-}C_6H_3(CF_3)_2)_4^-$ (BAr_f^-), are incorporated to provide solubility in organic solvents, as the hydrogen bond donor sites could become "saturated" or less accessible to substrates in water or other hydrogen bond accepting solvents.

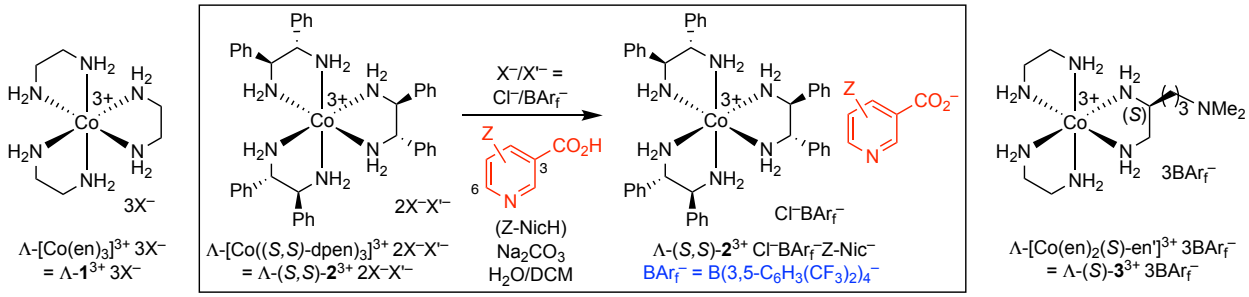

Figure 2.1. Monofunctional and bifunctional cobalt(III) hydrogen bond donor catalysts relevant to this study.

[†]Reprinted with permission from "Solvent free enantioselective catalysis with chiral cobalt(III) Werner complexes via ball milling" by Kabes, C. Q.; Jameson, B. L.; Gladysz, J. A. *New J. Chem.* **2021**, *45*, 17101−17107. from the Royal Society of Chemistry.

Related species with three chiral (*S*,*S*)- or (*R*,*R*)-1,2-diphenylethylenediamine ligands, [Co(dpen)$_3$]$^{3+}$ (see (*S*,*S*)-**2**$^{3+}$ in Figure 2.1), have proved to be especially effective enantioselective catalysts for a variety of reactions typically conducted in acetone, acetonitrile, or dichloromethane.[10,14,15] Both dpen enantiomers are commercially available at surprisingly low prices,[16] and all cobalt/carbon diastereomers (Co_Δ/Co_Λ versus $6C_R/6C_S$) are easily obtained. Most of these transformations require catalytic quantities of tertiary amine bases, although stoichiometric amounts are often employed. In a complementary effort, single component bifunctional catalysts were prepared in which a tertiary amine base was incorporated into the trication, as exemplified by Λ-(*S*)-**3**$^{3+}$ in Figure 2.1.[17] This gave higher enantioselectivities than the best systems with external bases, but required a lengthy synthesis including a chromatographic diastereomer separation.

Very recently, other bifunctional cobalt(III) catalysts have been developed that are much improved from the accessibility and sustainability standpoints.[15] As shown in Figure 2.1, these are based upon [Co(*S*,*S*-dpen)$_3$]$^{3+}$ ((*S*,*S*)-**2**$^{3+}$), but now feature a counter anion into which a nitrogen donor base has been incorporated. Initial experiments used the pyridine-based nicotinate anion (Nic$^-$), but a variety of substituted nicotinic as well as isonicotinic acids are commercially available. Among their conjugate bases, the 6-aminonicotinate anion (H_2N-Nic$^-$) was the top performer. Importantly, catalysts that featured combinations of chloride and BAr_f^- anions and an external pyridine base were ineffective, even with stoichiometric quantities of pyridine.[15]

Given the capability to generate numerous single component bifunctional cobalt(III) catalysts via a simple "drop in" counter anion strategy, it seemed an appropriate time to scout for still "greener" protocols. Accordingly, we sought to study the feasibility of applying the boxed sets of catalysts in Figure 2.1 under solvent free conditions in an inexpensive rudimentary ball mill of a type commonly available in many laboratories. As detailed below, excellent results have been obtained with respect to both rates and enantioselectivities, highlighting the very promising futures of these catalyst families and providing impetus for further development.

2.2. Results

2.2.1 Test reaction, apparatus, and preliminary screening. The Michael addition of dimethylmalonate (**4**) to *trans*-β-nitrostyrene (**5a**) shown in Figure 2.2A has been used as a test or benchmark reaction for a variety of cobalt(III) hydrogen bond donor catalysts,[10] even beyond the types shown in Figure 2.1.[18] There is an extensive body of data for $[Co((S,S)\text{-dpen})_3]^{3+}$ $2Cl^-BAr_f^-$ and analogs with related halide, pseudohalide, and tetraarylborate anions.[14a] The best catalysts afford the product **6a** in >90% ee and 90% yields after a few hours at room temperature at 10% loadings. For reasons not fully understood, the tetrafluoroborate salt $[Co((S,S)\text{-dpen})_3]^{3+}$ $3BF_4^-$ often gives marginally higher enantioselectivities.[14a]

For this study, **4** and **5a** were combined in disposable milling vials containing three meth-acrylate balls in the apparatus shown in Figure 2.2C, and under various conditions described below. After 30 minutes of milling at ambient temperatures, the samples usually exhibited an oily constitution. They were then taken up in a deuterated solvent containing a known quantity of an internal standard and analyzed by ^1H NMR and chiral HPLC. The milling process generates a moderate amount of heat, as does the motor, the effect of which is analyzed in control experiments below.

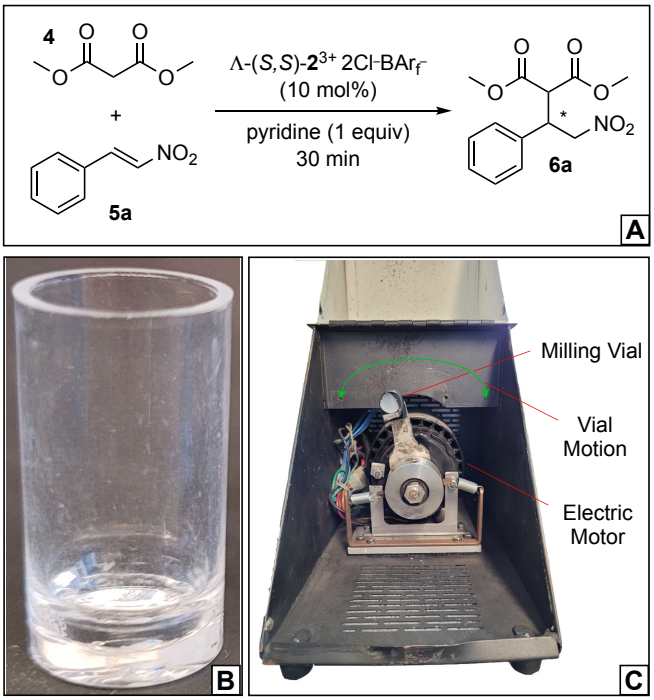

Figure 2.2. The conversion of dimethyl malonate (**4**) and *trans*-β-nitrostyrene (**5a**) to product **6a** (**A**) is carried out with a ball mill (**C**) that features a polystyrene vial (**B**) attached to an oscillating arm moved by an electric motor.

Experiments with monofunctional catalysts were conducted first. As shown in entry 2 of Table 1, the catalyst Λ-(*S*,*S*)-$\mathbf{2}^{3+}$ $2Cl^{-}BAr_f^{-}$ (10 mol%) was combined with a 1:1:1 mol ratio of **4**, **5a**, and the base triethylamine. After milling for 30 min, NMR and HPLC analyses indicated a 99% yield of **6a**, but the ee value was only 44%, versus 87% under standard conditions in acetone at 0 °C.[14a] When the base was omitted, only a 10% yield of **6a** was obtained (entry 1), and when the catalyst was omitted, no conversion occurred.

When triethylamine was replaced by *N*-methylmorpholine (NMM), the ee value significantly increased (67%; entry 3). Pyridine, which is commonly inferior to triethylamine in acetone and other solvents, afforded a higher ee yet (77%, entry 4). The pK_a (BH^+) values decrease from 10.7 to 7.1 to 5.2 in this series.[19] However, when the still weaker base 3-bromopyridine was tested (pK_a(BH^+) 2.9), both the yield and enantioselectivity decreased (entry 5). In all experiments giving lower yields of **6a**, considerable quantities of **4** and **5a** remained, but this was difficult to quantify due to impurities extracted from the disposable milling vials.

Table 2.1. Comparison of bases for the enantioselective addition of dimethyl malonate (**4**) to *trans*-β-nitrostyrene (**5a**).

entry	catalyst[a]	base	ee (%) (config)[b]	yield (%)[c]
1	Λ-(*S*,*S*)-$\mathbf{2}^{3+}$ 2Cl$^-$BAr$_f^-$	-	-	10
2	Λ-(*S*,*S*)-$\mathbf{2}^{3+}$ 2Cl$^-$BAr$_f^-$	Et_3N	44 (*R*)	99
3[d]	Λ-(*S*,*S*)-$\mathbf{2}^{3+}$ 2Cl$^-$BAr$_f^-$	NMM	67 (*R*)	99
4	Λ-(*S*,*S*)-$\mathbf{2}^{3+}$ 2Cl$^-$BAr$_f^-$	Py	77 (*R*)	96
5	Λ-(*S*,*S*)-$\mathbf{2}^{3+}$ 2Cl$^-$BAr$_f^-$	3-BrPy	53 (*R*)	15
6	Λ-(*S*,*S*)-$\mathbf{2}^{3+}$ 2Cl$^-$BAr$_f^-$	*rac*-$PhCH_2NH_2CH_3$	55 (*R*)	99
7	Λ-(*S*,*S*)-$\mathbf{2}^{3+}$ 2Cl$^-$BAr$_f^-$	(*S*)-$PhCH_2NH_2CH_3$	57 (*R*)	99
8	Λ-(*S*,*S*)-$\mathbf{2}^{3+}$ 2Cl$^-$BAr$_f^-$	(*S*)-4-PyCH(OH)CH_3	76 (*R*)	90
9	Λ-(*S*,*S*)-$\mathbf{2}^{3+}$ 2Cl$^-$BAr$_f^-$	(*R*)-2-PyCH(OH)CH_3	71 (*R*)	59
10	Λ-(*S*,*S*)-$\mathbf{2}^{3+}$ 3Cl$^-$	Et_3N	30 (*R*)	50

[a]Reactions were conducted for 30 min according to the general procedure with **5a** (0.060 mmol), catalyst (10 mol%), base (0.060 mmol), and **4** (0.066 mmol). [b]Determined by Chiral HPLC. [c]Determined by ^{1}H NMR relative to the internal standard Ph_2SiMe_2. [d]20 min reaction time.

Given the ease of catalyst screening, a few experiments deviating from the main thrust of this work were carried out. Entries 6 and 7 of Table 2.1 feature the chiral base 1-phenethylamine (pK_a(BH$^+$) 9.5). However, both racemic (entry 6) and enantiopure (entry 7) bases gave similar results (99% yields, 55–57% ee), showing that in these cases, the cobalt trication sets the degree of asymmetric induction.[20] Two isomeric enantiopure pyridylethanols were also evaluated (entries 8, 9; pK_a(BH$^+$) 5.3–5.7), but gave results slightly inferior to those with pyridine.

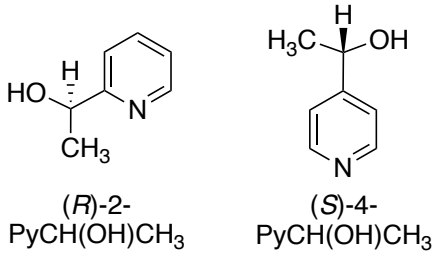

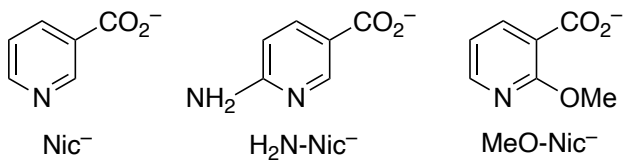

Figure 2.3. Pyridine containing bases or anions employed.

The final experiment in Table 2.1 (entry 10) features the trichloride salt that is the precursor to all Λ configured cobalt(III) catalysts in this paper. Since it is insoluble in aprotic organic solvents, its activity could not heretofore be tested under comparable conditions. The data show it to be inferior from the standpoints of both yield and enantioselectivity.[21]

2.2.2. Second set of screening reactions. In the next series of experiments, various pyridine containing systems were investigated, always with 10 mol% catalyst loadings. In entries 1-3 of Table 2.2, different salts of the trication Λ-(*S*,*S*)-$\mathbf{2}^{3+}$ were combined with a 1:1:1 mol ratio of **4**, **5a**, and pyridine. The counter anions can clearly have significant effects upon yields and enantiomeric excesses. Simply changing the chloride anions in Λ-(*S*,*S*)-$\mathbf{2}^{3+}$ $2Cl^{-}BAr_f^{-}$ to bromide and then tetrafluoroborate anions reduced the yields from 96% to 58% to 36% and the ee values from 77% to 71% to 56%. This parallels the diminishing hydrogen bond acceptor strengths of these anions.[22]

As shown in entries 4 and 5, the tris(borate) salts Λ-(*S*,*S*)-$\mathbf{2}^{3+}$ $3BF_4^{-}$ and Λ-(*S*,*S*)-$\mathbf{2}^{3+}$ $3BAr_f^{-}$, which are related to the mixed salt Λ-(*S*,*S*)-$\mathbf{2}^{3+}$ $2BF_4^{-}BAr_f^{-}$ in entry 3, afforded still poorer enantioselectivities. Finally, the opposite diastereomer Δ-(*S*,*S*)-$\mathbf{2}^{3+}$ $2Cl^{-}BAr_f^{-}$ gave an excellent yield, but the ee value was lower than that in entry 1 (50% vs. 77%) and the dominant configuration of **6a** was inverted (*S*). This paralleled the trend usually observed with $Co_{\Delta}/6C_S$ and $Co_{\Lambda}/6C_S$ catalyst diastereomers in solution.[14a]

Table 2.2. Comparison of catalysts for the enantioselective addition of dimethyl malonate (**4**) to *trans*-β-nitrostyrene (**5a**).

entry	catalyst[a]	base	ee (%) (config)[a]	yield (%)[a]
1a	Λ-(*S*,*S*)-**2**$^{3+}$ 2Cl$^-$BAr$_f^-$	Py	77 (*R*)	96
1b[b]	Λ-(*S*,*S*)-**2**$^{3+}$ 2Cl$^-$BAr$_f^-$	Py	77 (*R*)	96
2	Λ-(*S*,*S*)-**2**$^{3+}$ 2Br$^-$BAr$_f^-$	Py	71 (*R*)	58
3	Λ-(*S*,*S*)-**2**$^{3+}$ 2BF$_4^-$BAr$_f^-$	Py	56 (*R*)	36
4	Λ-(*S*,*S*)-**2**$^{3+}$ 3BAr$_f^-$	Py	46 (*R*)	95
5	Λ-(*S*,*S*)-**2**$^{3+}$ 3BF$_4^-$	Py	48 (*R*)	31
6	Δ-(*S*,*S*)-**2**$^{3+}$ 2Cl$^-$BAr$_f^-$	Py	50 (*S*)	99
7a	Λ-(*S*,*S*)-**2**$^{3+}$ Cl$^-$BAr$_f^-$Nic$^-$	-	73 (*R*)	67
7b[c]	Λ-(*S*,*S*)-**2**$^{3+}$ Cl$^-$BAr$_f^-$Nic$^-$	-	74(*R*)	81
8	Λ-(*S*,*S*)-**2**$^{3+}$ Cl$^-$BAr$_f^-$H$_2$N-Nic$^-$	-	70 (*R*)	99
9	Λ-(*S*,*S*)-**2**$^{3+}$ Cl$^-$BAr$_f^-$MeO-Nic$^-$	-	68 (*R*)	99

[a]These reactions and analyses thereof were conducted analogously to those in Table 1. [b]To help dissipate heat (see text) a 20 min milling period was followed by a 20 min pause and then another 20 min milling period. [c]This run was conducted as in entry 1b but with 15 min milling periods and pauses.

Entries 7–9 in Table 2.2 involve the single component bifunctional catalysts Δ-(*S*,*S*)-**2**$^{3+}$ Cl$^-$BAr$_f^-$Z-Nic$^-$ introduced in Figure 2.3. These feature Z = H, H$_2$N (6-position) and MeO (2 position), respectively (Figure 2.3). The ee values were close to the best (73–68% ee), but the yields were higher with the substituted nicotinates (99% versus 67% for Z = H). Accordingly, (*S*,*S*)-**2**$^{3+}$ Cl$^-$BAr$_f^-$H$_2$N-Nic$^-$, which was distinctly superior for the corresponding reactions in acetone,[15] was included in additional experiments below.

2.2.3. Other reaction parameters. The kinetic energy associated with milling can generate noticeable levels of heat.[23] Furthermore, the reaction vessel in Figure 2.2B warms to ca. 50 °C over the course of 30 min due to the radiant heat of the motor. As one probe of possible temperature effects, the reactions were carried out over two ca. 15 min intervals, separated by a comparable "cool down" window. As shown in entries 1b and 7b of Table 2.2, essentially identical enantioselectivities were obtained.

As summarized in Table 2.3, the catalyst loadings (entries 1–5), reaction times (entries 6–8), number of milling balls (entries 9–11), and reaction scales (entries 13–15) were also varied.

Most of these runs were conducted with Λ-(*S*,*S*)-$\mathbf{2}^{3+}$ 2Cl$^-$BAr$_f^-$/pyridine, the catalyst system judged best in Tables 2.1 (entry 4) and 2 (entry 1a). With regard to loading, one relevant factor briefly noted above is that when the yield of **6a** is not quantitative, unreacted **4** and **5a** always remain. Thus, given that enantioselectivities are not adversely affected at 5% loadings (entries 1 and 4), it is a simple matter to enhance yields by increasing reaction times. This is further supported by entries 6–8, which document the increase of yield with time under closely related conditions.

Table 2.3. Exploration of additional variables in the enantioselective addition of dimethyl malonate (**4**) to *trans*-β-nitrostyrene (**5a**).[a,b]

entry	catalyst[a]	variable	ee (%) (config)[a]	yield (%)[a]
1	Λ-(*S*,*S*)-$\mathbf{2}^{3+}$ 2Cl$^-$BAr$_f^-$	5% loading	76 (*R*)	70
2[c]	Λ-(*S*,*S*)-$\mathbf{2}^{3+}$ 2Cl$^-$BAr$_f^-$	10% loading	77 (*R*)	96
3	Λ-(*S*,*S*)-$\mathbf{2}^{3+}$ 2Cl$^-$BAr$_f^-$	15% loading	74 (*R*)	93
4[b]	Λ-(*S*,*S*)-$\mathbf{2}^{3+}$ Cl$^-$BAr$_f^-$Nic-NH$_2^-$	5% loading	73 (*R*)	70
5[b]	Λ-(*S*,*S*)-$\mathbf{2}^{3+}$ Cl$^-$BAr$_f^-$Nic-NH$_2^-$	10% loading	70 (*R*)	99
6	Λ-(*S*,*S*)-$\mathbf{2}^{3+}$ 2Cl$^-$BAr$_f^-$	10 min time	76 (*R*)	62
7	Λ-(*S*,*S*)-$\mathbf{2}^{3+}$ 2Cl$^-$BAr$_f^-$	20 min time	72 (*R*)	97
8[c]	Λ-(*S*,*S*)-$\mathbf{2}^{3+}$ 2Cl$^-$BAr$_f^-$	30 min time	77 (*R*)	96
9a	Λ-(*S*,*S*)-$\mathbf{2}^{3+}$ 2Cl$^-$BAr$_f^-$	0 balls	38 (*R*)	78
9b[c]	Λ-(*S*,*S*)-$\mathbf{2}^{3+}$ 2Cl$^-$BAr$_f^-$	0 balls	48 (*R*)	15
10	Λ-(*S*,*S*)-$\mathbf{2}^{3+}$ 2Cl$^-$BAr$_f^-$	2 balls	76 (*R*)	98
11[c]	Λ-(*S*,*S*)-$\mathbf{2}^{3+}$ 2Cl$^-$BAr$_f^-$	3 balls	77 (*R*)	96
12	Λ-(*S*,*S*)-$\mathbf{2}^{3+}$ 2Cl$^-$BAr$_f^-$	4 balls	73 (*R*)	99
13	Λ-(*S*,*S*)-$\mathbf{2}^{3+}$ 2Cl$^-$BAr$_f^-$	0.5 scale	69 (*R*)	85
14[c]	Λ-(*S*,*S*)-$\mathbf{2}^{3+}$ 2Cl$^-$BAr$_f^-$	1 scale (normal)	77 (*R*)	96
15	Λ-(*S*,*S*)-$\mathbf{2}^{3+}$ 2Cl$^-$BAr$_f^-$	1.5 scale	73 (*R*)	95

[a]These reactions and analyses thereof were conducted analogously to those in Table 2.1, except for the variation noted. [b]All entries except 4 and 5 are carried out in the presence of pyridine (equimolar with **4** and **5a**). [c]These represent identical experiments. [c]In this experiment, the reaction vessel was not attached to the oscillating arm in Figure 2.2C, and instead kept as motionless as possible.

Entries 9–12 of Table 2.3 show that as long as there are at least two milling balls, yields and enantioselectivities remain constant. However, differences might have been noted if data had been acquired at shorter time intervals. It might at first seem surprising that significant conversions

can be realized in the absence of milling balls, albeit with lower enantioselectivities (entry 9a). In fact, vigorous shaking alone can provide a sufficient mechanochemical driving force. Importantly, in the absence of physical agitation, reaction essentially ceases (entry 9b). In the reaction scale experiments (entries 13–15), the molar quantities of **4** and **5a** are increased or decreased within the same overall volume. Both the rates and enantioselectivities decrease slightly at the lowest vessel loading. Perhaps reactant contact becomes suboptimal if the vessel is too empty or overfilled.

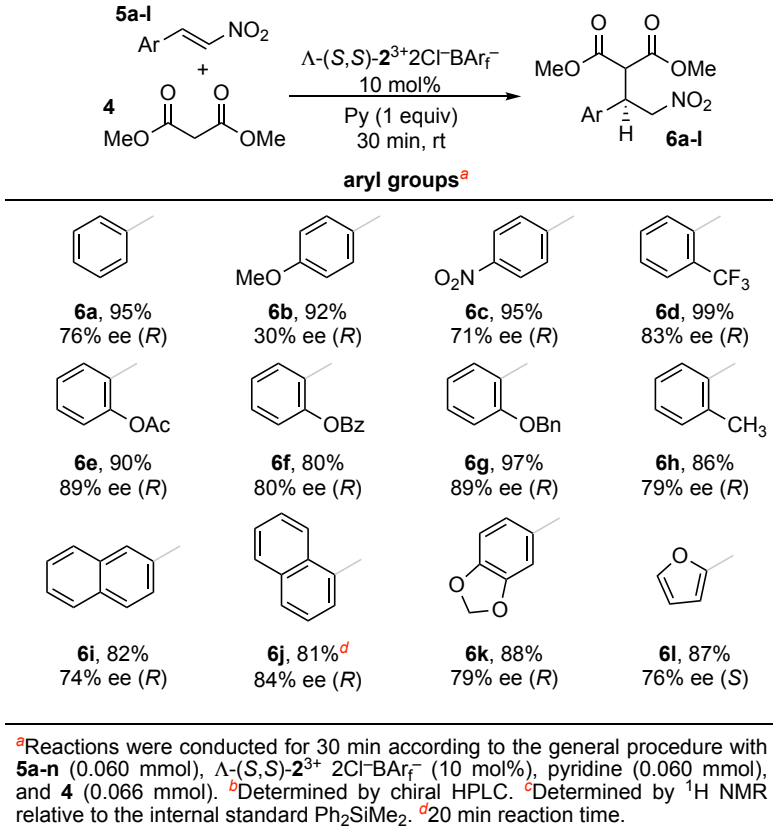

[a]Reactions were conducted for 30 min according to the general procedure with **5a-n** (0.060 mmol), Λ-(*S*,*S*)-**2**$^{3+}$ 2Cl^{-}BAr$_f^{-}$ (10 mol%), pyridine (0.060 mmol), and **4** (0.066 mmol). [b]Determined by chiral HPLC. [c]Determined by ^{1}H NMR relative to the internal standard Ph_2SiMe_2. [d]20 min reaction time.

Chart 2.1. Substrate scope for the enantioselective addition of dimethyl malonate (**4**) to *trans* 2-aryl 1-nitroethylenes.

2.2.4. Substrate scope. Given the slightly better performance of the Λ-(*S*,*S*)-**2**$^{3+}$ 2Cl^{-}BAr$_f$ /pyridine catalyst system as compared to bifunctional Λ-(*S*,*S*)-**2**$^{3+}$ Cl^{-}BAr$_f^{-}$H$_2$N-Nic^{-} in Table 2.2 (77% vs. 70% ee), the substrate scope was mainly explored with the former, always applying the optimal conditions from Table 2.3. As summarized in Chart 2.1, twelve nitroolefins (**5a–l**) were evaluated. These gave the addition products (**6a–l**) in average yields and ee values of 89% and 74% (median ee 80%). The dominant absolute configurations of most adducts could be assigned

by previously established chiral HPLC relationships, as documented in the supporting information. These always corresponded to the same relative configurations. Thus, for the two cases for which HPLC assignments have not yet been established (**6c**,**h**), identical relative configurations were presumed.

The nitroolefins **5e**,**f**,**i** were also evaluated with the bifunctional catalyst Λ-(*S*,*S*)-$\mathbf{2}^{3+}$ Cl^- $BAr_f^-H_2N$-Nic^- under analogous conditions but in the absence of pyridine, giving **6e**,**f**,**i** in comparable enantioselectivities (83%, 83%, 73% ee). When **5a** was treated with di*ethyl* malonate in place of **4** in Chart 2.1, the yield of the addition product remained high (94%) while the ee dropped (54%).

2.3 Discussion

The preceding efforts have established the feasibility of applying several types of chiral cobalt(III) hydrogen bond donor catalysts under solvent free conditions through the agency of mechanochemistry. Our ball milling protocols significantly reduce reaction times, and can also alter the order of catalyst effectiveness. One conspicuous example involves entries 2 and 4 of Table 2.1. In organic solvents, Λ-(*S*,*S*)-$\mathbf{2}^{3+}$ $2Cl^-BAr_f^-$/triethylamine gives much higher enantioselectivities than Λ-(*S*,*S*)-$\mathbf{2}^{3+}$ $2Cl^-BAr_f^-$/pyridine,[15] but with ball milling pyridine is the superior base. A recent review describes several possible origins of such phenomena.[7]

One concern is that ball milling seemingly gives slightly lower enantioselectivities. For example, the average ee value in Chart 2.1 (74%) is less than that for the same twelve nitroolefins with the single component catalyst Λ-(*S*,*S*)-$\mathbf{2}^{3+}$ $Cl^-BAr_f^-H_2N$-Nic^- (86%; acetone, 0 °C),[15] or that for the eight nitroolefins that have been similarly assayed with Λ-(*S*,*S*)-$\mathbf{2}^{3+}$ $2Cl^-BAr_f^-$/triethylamine (89%; acetone, 0 °C).[14a] One factor is likely the temperature differential –0 °C versus the moderate heat generated during ball milling.[23] Accordingly, second generation efforts that use cooled or thermostated ball mills may deliver improved results. However, there are additional possible contributing factors.[7] For example, given the relatively common solvent effects upon enantioselectivities, "no solvent" effects are also to be expected.

The physical state of the samples employed in Tables 2.1–2.3 also deserves emphasis.

Whereas *trans*-ß-nitrostyrene (**5a**) is a solid (mp 58 °C), dimethyl malonate (**4**) is a liquid (freezing point –62 °C). All of the catalysts are solids, but all of the bases employed except for the hydroxylated pyridines (Figure 2.3) are liquids. Thus, all experiments begin with what can be termed a "wetted solid". In no case does ball milling produce a free flowing homogeneous solution, but as noted above most reaction mixtures have a very oily constitution.

Mechanochemistry has also been applied to purely organic hydrogen bond donor catalysts.[24–26] Of particular relevance are reports detailing additions of 1,3-dicarbonyl compounds (diketones, ß-oxoesters, dimethyl malonate) to nitroolefins using chiral squaramide[24] or thiourea[25] catalysts. Additions of additional types of acidic C–H units have also been reported.[26] Other research groups are developing cobalt(III) based hydrogen bond donor catalysts,[11,27] but solvent free protocols remain to be reported.

Although Table 2.3 illustrates some of the mechanochemically related variables that can affect yields and enantioselectivities, Tables 2.1 and 2.2 as well as earlier published work[10] drive home the point that catalyst design remains the key challenge for further optimization. Due to the many NH hydrogen bond donor units in each catalyst molecule (twelve versus two for thiourea), it has remained challenging to formulate detailed mechanisms or otherwise rationalize the counter anion trends so evident in Table 2.2 and previous studies. The cobalt trications present two "C_3 symmetric faces" and three "C_2 symmetric faces", and either or even combinations of adjacent faces may play roles in activating the educts.

2.4 Conclusion

In summary, this work has established that the cobalt(III) catalysts developed in this laboratory can be applied in solvent free mechanochemical protocols. There are fascinating changes in the relative performances of these catalysts under the new ball milling conditions. Although the enantioselectivities apparently diminish somewhat, there are possible remedies that will be explored in future research. The synthesis and evaluation of related catalyst families remain under intense investigation and additional developments will be reported by future coworkers.

2.5 Experimental

General: All reactions and workups were conducted in air. NMR spectra were recorded on standard FT spectrometers at ambient probe temperatures. Chemical shifts (δ/ppm) were referenced to solvent signals (^{1}H: acetone-d_5, 2.05; CHD_2CN, 1.94; ^{13}C: acetone-d_6, 29.8; CD_3CN, 1.32). Microanalyses were conducted by Atlantic Microlab. HPLC analyses employed a Shimadzu instrument package (pump/autosampler/detector LC-20AD/SIL-20A /SPD-M20A).

Reactions were carried out using a SPEX CertiPrep 5100 mixer-mill, SPEX 3111 polystyrene grinding vials, and SPEX 3119 methacrylate balls (1/8 in). Catalysts were synthesized according to published procedures.[14a,15,28] The 1-phenylethylamine (Alfa Aesar, 98%), 1-(*S*)-phenylethylamine (Aldrich, 98%), (*S*)-(4-pyridyl)ethanol (Ambeed, 98+%), and (*R*)-(2-pyridyl)ethanol (Ambeed, 95+%) were used as received. Solvents and routine chemicals were obtained as reported earlier.[15]

Typical Procedure for Nitroolefin Addition in Ball Mill: A polystyrene grinding vial (Figure 2.2B) was charged with *trans*-β-nitrostyrene (**5a**; 0.0090 g, 0.060 mmol, 1.0 equiv), dimethyl malonate (**4**, 0.0076 mL, 0.066 mmol, 1.1 equiv), Ph_2SiMe_2 (0.0013 mL, internal standard), pyridine (0.0049 mL, 0.060 mmol, 1.0 equiv), and Λ-(*S*,*S*)-**1**$^{3+}$ 2$Cl^-BAr_f^-$·2H_2O (0.0102 g, 0.0060 mmol, 10 mol%).[28] Three milling balls were added and the vial was capped. The sample was milled for 30 minutes. The residue was dissolved in acetone-d_6 and immediately assayed via ^{1}H NMR. The solvent was removed by rotary evaporation and the residue chromatographed on silica (glass pipette, 25:75 v/v EtOAc/hexanes). The solvent was removed from the product containing fractions by rotary evaporation to give **6a** as a colorless oil (96%). Enantiomeric excesses were determined by HPLC with a Chiralcel AD column (98:2 v/v hexane/isopropanol, 1 mL/min, λ = 220 nm); t_R = 33.3 min (major), 43.4 min (minor), 76% ee.[14a]

NMR ($CDCl_3$, δ/ppm): ^{1}H (400 MHz) 7.36–7.27 (m, 3H), 7.25–7.19 (m, 2H), 4.93 (dd, $^2J_{HH}$ = 13.3 Hz, $^3J_{HH}$ = 5.4 Hz, 1H), 4.88 (dd, $^2J_{HH}$ = 13.3 Hz, $^3J_{HH}$ = 8.8 Hz, 1H), 4.24 (td, $^3J_{HH}$

= 8.9 Hz, $^{3}J_{HH}$ = 5.3 Hz, 1H), 3.86 (d, $^{3}J_{HH}$ = 9.0 Hz, 1H), 3.76 (s, 3H), 3.56 (s, 3H); $^{13}C\{^{1}H\}$ (100 MHz) 168.0, 167.4, 136.3, 129.2, 128.6, 128.0, 77.5, 54.9, 53.2, 53.0, 43.0 (11 × s).

Nitroolefin substrate scope (Chart 2.1): These experiments were carried out analogously to those in Tables 2.1 and 2.2, and gave products previously reported in the literature as colorless oils.[15]

Dimethyl 2-(2-nitro-1-(4-methoxyphenyl)ethyl)malonate (6b). This known compound was obtained as a colorless oil, 92%. NMR ($CDCl_3$, δ/ppm): ^{1}H 7.19–7.09 (m, 2H), 6.88–6.76 (m, 2H), 4.89 (dd, $^{2}J_{HH}$ = 13.0 Hz, $^{3}J_{HH}$ = 5.0 Hz, 1H), 4.83 (dd, $^{2}J_{HH}$ = 13.0 Hz, $^{3}J_{HH}$ = 9.2 Hz, 1H), 4.19 (td, $^{3}J_{HH}$ = 9.1, 5.0 Hz, 1H), 3.83 (d, $^{3}J_{HH}$ = 9.2 Hz, 1H), 3.77 (s, 3H), 3.76 (s, 3H), 3.57 (s, 3H); $^{13}C\{^{1}H\}$ 168.0, 167.4, 159.6, 129.1, 128.0, 114.5, 77.8, 55.4, 55.0, 53.1, 53.0, 42.5 (12 × s). The enantiomer excess was determined by HPLC with a Chiralcel AD column (80:20 v/v hexane/isopropanol, 1 mL/min, λ = 254 nm); t_R = 11.4 min (major), 17.0 min (minor), 30% ee.[14a]

Dimethyl 2-(2-nitro-1-(4-nitrophenyl)ethyl)malonate (6c). This known compound was obtained as a colorless oil, 95%. NMR ($CDCl_3$, δ/ppm): ^{1}H 8.27–8.00 (m, 2H), 7.56–7.37 (m, 2H), 4.97 (dd, $^{2}J_{HH}$ = 13.7 Hz, $^{3}J_{HH}$ = 5.3 Hz, 1H), 4.92 (dd, $^{2}J_{HH}$ = 13.7 Hz, $^{3}J_{HH}$ = 8.9 Hz, 1H), 4.37 (td, $^{3}J_{HH}$ = 8.9, 5.1 Hz, 1H), 3.88 (d, $^{3}J_{HH}$ = 8.8 Hz, 1H), 3.78 (s, 3H), 3.61 (s, 3H); $^{13}C\{^{1}H\}$ 167.3, 166.7, 143.5, 129.1, 124.2, 76.6, 54.1, 53.3, 53.2, 42.5 (10 × s). The enantiomer excess was determined by HPLC with a Chiralcel OD-H column (80:20 v/v hexane/isopropanol, 1 mL/ min, λ = 220 nm); t_R = 21.2 min (minor), 32.5 min (major), 71% ee.[17]

Dimethyl 2-(2-nitro-1-(2-trifluoromethylphenyl)ethyl)malonate (6d). This known compound was obtained as a colorless oil, 99%. ^{1}H NMR ($CDCl_3$, δ/ppm): 7.75–7.66 (m, 1H), 7.60–7.48 (m, 1H), 7.47–7.39 (m, 1H), 7.37 (d, $^{3}J_{HH}$ = 7.9 Hz, 1H), 5.16 (dd, $^{2}J_{HH}$ = 13.4 Hz, $^{3}J_{HH}$ = 7.6 Hz, 1H), 4.94 (dd, $^{2}J_{HH}$ = 13.4 Hz, $^{3}J_{HH}$ = 4.5 Hz, 1H), 4.65 (td, $^{3}J_{HH}$ = 7.5, 4.5 Hz, 1H), 4.11 (d, $^{3}J_{HH}$ = 7.4 Hz, 1H), 3.75 (s, 3H), 3.64 (s, 3H). The enantiomer excess was determined by HPLC with a Chiralcel OD column (95:5 v/v hexane/isopropanol, 1 mL/min, λ = 220 nm); t_R = 11.6 min (minor), 21.9 min (major), 83% ee.[14a]

Dimethyl 2-(2-nitro-1-(2-acetoxyphenyl)ethyl)malonate (6e). This known compound was obtained as a colorless oil, 90%. NMR ($CDCl_3$, δ/ppm): ^1H (400 MHz) 7.28–7.04 (m, 4H), 4.86 (dd, $^2J_{HH}$ = 13.3 Hz, $^3J_{HH}$ = 7.6 Hz, 1H), 4.81 (dd, $^2J_{HH}$ = 13.3 Hz, $^3J_{HH}$ = 8.6 Hz, 1H), 4.43 (td, $^3J_{HH}$ = 8.2, 5.5 Hz, 1H), 3.85 (d, $^3J_{HH}$ = 8.5 Hz, 1H), 3.69 (s, 3H), 3.47 (s, 3H), 2.37 (s, 3H); $^{13}C\{^1H\}$ 169.2, 168.0, 167.4, 148.7, 129.4, 128.5, 128.2, 126.5, 123.5, 76.5, 53.8, 53.1 (double intensity), 36.7, 21.2 (14 × s). The enantiomer excess was determined by HPLC with a Chiralcel OD column (90:10 v/v hexane/isopropanol, 1 mL/min, λ = 210 nm); t_R = 16.9 min (minor), 24.6 min (major), 89% ee.[14a]

Dimethyl 2-(2-nitro-1-(2-benzoyloxyphenyl)ethyl)malonate (6f). This known compound was obtained as a colorless oil, 80%. NMR ($CDCl_3$, δ/ppm): ^1H 8.36–8.20 (m, 2H), 7.74–7.64 (m, 1H), 7.60–7.52 (m, 2H), 7.42–7.31 (m, 2H), 7.30–7.22 (m, 2H), 4.98 (dd, $^2J_{HH}$ = 13.5 Hz, $^3J_{HH}$ = 8.5 Hz, 1H), 4.91 (dd, $^2J_{HH}$ = 13.6 Hz, $^3J_{HH}$ = 4.9 Hz, 1H), 4.59 (td, $^3J_{HH}$ = 8.6, 4.9 Hz, 1H), 3.96 (d, $^3J_{HH}$ = 8.5 Hz, 1H), 3.72 (s, 3H), 3.53 (s, 3H); $^{13}C\{^1H\}$ 168.0, 167.4, 164.9, 149.0, 134.1, 130.4, 129.5, 129.1, 129.0, 128.7, 128.3, 126.6, 123.6, 76.6, 53.9, 53. 1, 53.1, 36.7 (18 × s). The enantiomer excess was determined by HPLC with a Chiralcel AD column (90:10 v/v hexane/ isopropanol, 1 mL/min, λ = 220 nm); t_R = 15.5 min (major), 24.7 min (minor), 80% ee.[14a]

Dimethyl 2-(2-nitro-1-(2-benzyloxyphenyl)ethyl)malonate (6g). This known compound was obtained as a colorless oil, 97%. NMR ($CDCl_3$, δ/ppm): ^1H 7.51–7.45 (m, 2H), 7.45–7.40 (m, 2H), 7.39–7.33 (m, 1H), 7.24 (ddd, $^3J_{HH}$ = 8.3, 7.4 Hz, $^4J_{HH}$ = 1.7 Hz, 1H), 7.17 (dd, $^3J_{HH}$ = 7.6, $^4J_{HH}$ = 1.7 Hz, 1H), 6.93 (dd, $^3J_{HH}$ = 8.3, $^4J_{HH}$ = 1.1 Hz, 1H), 6.90 (td, $^3J_{HH}$ = 7.5 Hz, $^4J_{HH}$ = 1.1 Hz, 1H), 5.14 (d, $^2J_{HH}$ = 11.7 Hz, 1H), 5.11 (d, $^2J_{HH}$ = 11.7 Hz, 1H), 5.05 (dd, $^2J_{HH}$ = 13.0 Hz, $^3J_{HH}$ = 9.4 Hz, 1H), 4.84 (dd, $^2J_{HH}$ = 13.0 Hz, $^3J_{HH}$ = 4.6 Hz, 1H), 4.44 (td, $^3J_{HH}$ = 9.6, 4.6 Hz, 1H), 4.17 (d, $^3J_{HH}$ = 9.9 Hz, 1H), 3.72 (s, 3H), 3.50 (s, 3H); $^{13}C\{^1H\}$ 168.4, 167.7, 156.7, 136.6, 130.9, 129.8, 128.9, 128.4, 127.7, 123.9, 121.3, 112.5, 76.1, 70.7, 53.0, 52.7, 52.6, 40.5 (18 × s). The enantiomer excess was determined by HPLC with a Chiralcel OD column (90:10 v/v hexane/isopropanol, 1 mL/min, λ = 220 nm); t_R = 11.4 min (minor), 19.5 min (major), 89% ee.[14a]

Dimethyl 2-(2-nitro-1-(2-methylphenyl)ethyl)malonate (6h). This known compound was obtained as a colorless oil, 86%. NMR ($CDCl_3$, δ/ppm): ^{1}H 7.12–7.03 (m, 4H), 4.84 (dd, $^2J_{HH}$ = 13.6 Hz, $^3J_{HH}$ = 5.3 Hz, 1H), 4.78 (dd, $^2J_{HH}$ = 13.3 Hz, $^3J_{HH}$ = 8.6 Hz, 1H), 4.51 (td, $^3J_{HH}$ = 8.9, 5.4 Hz, 1H), 3.76 (d, $^3J_{HH}$ = 9.3 Hz, 1H), 3.68 (s, 3H), 3.52 (s, 3H), 2.33 (s, 3H); ^{13}C{^{1}H} 168.0, 167.3, 137.0, 134.5, 131.3, 128.1, 126.6, 125.8, 54.5, 53.0, 52.8, 52.6, 41.1, 37.7 (14 × s). The enantiomer excess was determined by HPLC with a Chiralcel AD-H column (90:10 v/v hexane/isopropanol, 1 mL/min, λ = 220 nm); t_R = 8.8 min (major), 15.3 min (minor), 79% ee.[29]

Dimethyl 2-(2-nitro-1-β-naphthylethyl)malonate (6i). This known compound was obtained as a colorless oil, 82%. ^{1}H NMR ($CDCl_3$, δ/ppm): 7.87–7.74 (m, 1H), 7.73–7.67 (m, 1H), 7.54–7.44 (m, 2H), 7.34 (dd, $^3J_{HH}$ = 8.5 Hz, $^4J_{HH}$ =1.9 Hz, 1H), 5.00 (d, $^3J_{HH}$ = 7.0 Hz, 2H), 4.43 (dt, $^3J_{HH}$ = 8.8, 7.0 Hz, 1H), 3.98 (d, $^3J_{HH}$ = 8.9 Hz, 1H), 3.77 (s, 3H), 3.54 (s, 3H). The enantiomer excess was determined by HPLC with a Chiralcel OD column (70:30 v/v hexane/isopropanol, 1 mL/min, λ = 254 nm); t_R = 12.5 min (major), 35.1 min (minor), 74% ee.[14a]

Dimethyl 2-(2-nitro-1-α-naphthylethyl)malonate (6j). This known compound was obtained as a colorless oil, 81%. ^{1}H NMR ($CDCl_3$, δ/ppm): 8.18 (d, $^3J_{HH}$ = 8.6 Hz, 1H), 7.98–7.85 (m, 1H), 7.84–7.73 (m, 1H), 7.62 (ddd, $^3J_{HH}$ = 8.5, 6.8 Hz, $^4J_{HH}$ = 1.4 Hz, 1H), 7.53 (ddd, $^3J_{HH}$ = 8.0, 6.8 Hz, $^4J_{HH}$ = 1.1 Hz, 1H), 7.46–7.34 (m, 2H), 5.29–5.20 (m, 1H), 5.18 (dd, $^2J_{HH}$ = 13.2 Hz, $^3J_{HH}$ = 8.2 Hz, 1H), 5.07 (dd, $^2J_{HH}$ = 13.1 Hz, $^3J_{HH}$ = 4.6 Hz, 1H), 4.11 (d, $^3J_{HH}$ = 7.6 Hz, 1H), 3.72 (s, 3H), 3.54 (s, 3H). The enantiomer excess was determined by HPLC with a Chiralcel AD column (90:10 v/v hexane/isopropanol, 1 mL/min, λ = 254 nm); t_R = 13.4 min (major), 18.0 min (minor), 84% ee.[14a]

Dimethyl 2-(2-nitro-1-(3,4-dioxolophenyl)ethyl)malonate (6k). This known compound was obtained as a colorless oil, 88%. NMR ($CDCl_3$, δ/ppm): ^{1}H 6.78–6.65 (m, 3H), 5.95 (s, 2H), 4.87 (dd, $^2J_{HH}$ = 13.1 Hz, $^3J_{HH}$ = 4.9 Hz, 1H), 4.80 (dd, $^2J_{HH}$ = 13.1 Hz, $^3J_{HH}$ = 9.3 Hz, 1H), 4.16 (td, $^3J_{HH}$ = 9.2, 4.9 Hz, 1H), 3.80 (d, $^3J_{HH}$ = 9.1 Hz, 1H), 3.77 (s, 3H), 3.61 (s, 3H); ^{13}C{^{1}H} 168.0, 167.3, 148.3, 147.8, 129.8, 121.5, 108.8, 208.3, 101.5, 77.7, 55.0, 53.2, 53.0, 42.9 (14 × s). The enantiomer excess was determined by HPLC with a Chiralcel AS-H column (90:10 v/v hex-

ane/isopropanol, 1 mL/min, λ = 220 nm); t_R = 39.5 min (major), 47.1 min (minor), 79% ee.[17]

Dimethyl 2-(2-nitro-1-furylethyl)malonate (6l). This known compound was obtained as a colorless oil, 87%. NMR ($CDCl_3$, δ/ppm): ^{1}H 7.35 (dd, $^3J_{HH}$ = 1.8 Hz, $^4J_{HH}$ = 0.6 Hz, 1H), 6.29 (dd, $^3J_{HH}$ = 3.3, 1.9 Hz, 1H), 6.22 (d, $^3J_{HH}$ = 3.3 Hz, 1H), 4.92 (dd, $^2J_{HH}$ = 13.5 Hz, $^3J_{HH}$ = 8.2 Hz, 1H), 4.86 (dd, $^2J_{HH}$ = 13.4 Hz, $^3J_{HH}$ = 5.1 Hz, 1H), 4.39 (td, $^3J_{HH}$ = 8.0, 5.1 Hz, 1H), 3.95 (d, $^3J_{HH}$ = 7.9 Hz, 1H), 3.76 (s, 3H), 3.70 (s, 3H); ^{13}C{^{1}H} 167.5, 167.2, 149.4, 142.9, 110.6, 108.5, 75.3, 53.1, 53.0, 52.7, 52.6 (11 × s). The enantiomer excess was determined by HPLC with a Chiralcel OD column (90:10 v/v hexane/isopropanol, 1 mL/min, λ = 220 nm); t_R = 10.9 min (minor), 22.5 min (major), 76% ee.[14a]

Diethyl 2-(2-nitro-1-phenylethyl)malonate (6a-Et). This known compound was obtained as a colorless oil, 94%. NMR ($CDCl_3$, δ/ppm): ^{1}H 7.44–7.12 (m, 5H), 4.92 (dd, $^2J_{HH}$ = 13.1 Hz, $^3J_{HH}$ = 4.8 Hz, 1H), 4.86 (dd, $^2J_{HH}$ = 13.1 Hz, $^3J_{HH}$ = 9.2 Hz, 1H), 4.31–4.16 (m, 3H), 4.01 (q, $^3J_{HH}$ = 7.1 Hz, 2H), 3.82 (d, $^3J_{HH}$ = 9.4 Hz, 1H), 1.26 (t, $^3J_{HH}$ = 7.1 Hz, 2H), 1.05 (t, $^3J_{HH}$ =7.1 Hz, 2H); ^{13}C{^{1}H} 167.6, 167.0, 136.4, 129.1, 128.5, 128.2, 77.8, 62.3, 62.0, 55.1, 43.1, 14.1, 13.9 (13 × s). The enantiomer excess was determined by HPLC with a Chiralcel AD column (90:10 v/v hexane/isopropanol, 1 mL/min, λ = 230 nm); t_R = 11.4 min (major), 24.3 min (minor), 54% ee.[30]

2.6 References. (All titles are given in the capitalization format of the original article)

(1) Tanaka, K.; Toda, F. Solvent-Free Organic Synthesis. *Chem. Rev.* **2000**, *100*, 1025–1074.

(2) Friščić, T.; Mottillo, C.; Titi, H. M. Mechanochemistry for Synthesis. *Angew. Chem. Int. Ed.* **2019**, *59*, 1018–1029; Mechanochemistry for Synthesis. *Angew. Chem.* **2020**, *132*, 1030–1041.

(3) Some journals have recently published thematic issues on this topic: (a) Hernández, J. G. Mechanochemistry. *Beilstein J. Org. Chem.* **2017**, *13*, 2372–2373. (b) The preceding Editorial introduces a special issue with 26 articles on the title subject. (c) Hernández, J. G. Mechanochemistry II. *Beilstein J. Org. Chem.* **2019**, *15*, 1521–1522. (d) The preceding Editorial introduces a special issue with 12 articles on the title subject.

(4) Stolle, A.; Szuppa, T.; Leonhardt, S. E. S.; Ondruschka, B. Ball milling in organic synthesis: solutions and challenges. *Chem. Soc. Rev.* **2011**, *40*, 2317–2329.

(5) Debecker, D. P.; Hi, K. K.; Moores, A.; Rossi, L. M.; Sels, B.; Allen, D. T.; Subramaniam, B. Shaping Effective Practices for Incorporating Sustainability Assessment in Manuscripts Submitted to ACS Sustainable Chemistry & Engineering: Catalysis and Catalytic Processes. *ACS Sustainable Chem. Eng.* **2021**, *9*, 4936–4940.

(6) See also Ardila-Fierro, K. J.; Hernández, J. G. Sustainability Assessment of Mechanochemistry by Using the Twelve Principles of Green Chemistry. *ChemSusChem* **2021**, *14*, 2145–2162.

(7) Egorov, I. N.; Santra, S.; Kopchuk, D. S.; Kovalev, I. S.; Zyryanov, G. V.; Majee, A.; Ranu, B. C.; Rusinov, V. L.; Chupakhin, O. N. Ball milling: an efficient and green approach for asymmetric organic synthesis. *Green Chem.* **2020**, *22*, 302–315.

(8) *Catalysis with Earth-abundant Element*s. Schneider, U.; Thomas, S. Eds. **2021**, Royal Society of Chemistry: London. ISBN: 978-1-78801-118-1.

(9) Shakespeare, W. *Macbeth*. **1606**, Act IV, Scene 1 (the first recorded dramatization of multicomponent recipes and by extrapolation catalysis).

(10) Wegener, A. R.; Kabes, C. Q.; Gladysz, J. A. Launching Werner Complexes into the Modern Era of Catalytic Enantioselective Organic Synthesis. *Acc. Chem. Res.* **2020**, *53*, 2299–2313.

(11) For related investigations involving other cobalt(III) or metal-containing hydrogen bond donor catalysts, see Larionov, V. A.; Feringa, B. L.; Belokon, Y. N. Enantioselective "organocatalysts in disguise" by the ligand sphere of chiral metal-templated complexes. *Chem. Soc. Rev.* **2021**, *50*, 9715–9740.

(12) Werner, A. Zur Kenntnis des asymmetrischen Kobaltatoms. V. *Ber. Dtsch. Chem. Ges.* **1912**, *45*, 121–130.

(13) As a historical aside, it should be noted that grinding operations have long been used in syntheses of certain cobalt(III) amine complexes: (a) Meisenheimer, J. Über Komplexverbin-

dungen des Chroms und Kobalts mit aliphatischen und aromatischen Aminen. *Annalen* **1924**, *438*, 217–278. (b) Bailar Jr., J. C.; Clapp, L. B. The Preparation and Properties of Cobalt Coordination Compounds. I. The Action of Some Organic Amines upon Dichloro-diethylenediamine Cobaltic Chloride. *J. Am. Chem. Soc.* **1945**, *67*, 171–175. (c) Buckingham, D. A.; Davis, C. E.; Sargeson, A. M. Cobalt(III)-Promoted Lysis at Saturated Carbon. Examples of Internal Nucleophilic Displacement. *J. Am. Chem. Soc.* **1970**, *92*, 6159–6170. (d) Buckingham, D. A.; Morris, P.; Sargeson, A. M.; Zanella, A. Intramolecular Hydration of Nitriles Coordinated to Cobalt(III). Formation of Five- and Six-Membered Chelated Amides. *Inorg. Chem.* **1977**, *16*, 1910–1923.

(14) (a) Lewis, K. G.; Ghosh, S. K.; Bhuvanesh, N.; Gladysz, J. A. Cobalt(III) Werner Complexes with 1,2-Diphenylethylenediamine Ligands: Readily Available, Inexpensive, and Modular Chiral Hydrogen Bond Donor Catalysts for Enantioselective Organic Synthesis. *ACS Cent Sci* **2015**, *1*, 50–56. (b) Kumar, A.; Ghosh, S. K.; Gladysz, J. A.; Tris(1,2-diphenylethylenediamine)cobalt(III) Complexes: Chiral Hydrogen Bond Donor Catalysts for Enantioselective α-Aminations of 1,3-Dicarbonyl Compounds. *Org. Lett.* **2016**, *18*, 760–763. (c) Joshi, H.; Ghosh, S. K.; Gladysz, J. A. Enantioselective Additions of Stabilized Carbanions to Imines Generated from α-Amido Sulfones By Using Lipophilic Salts of Chiral Tris(1,2-diphenylethylenediamine) Cobalt(III) Trications as Hydrogen Bond Donor Catalysts. *Synthesis* **2017**, *49*, 3905–3915. (d) Luu, Q. H.; Gladysz, J. A.; An Air- and Water-Stable Hydrogen-Bond-Donor Catalyst for the Enantioselective Generation of Quaternary Carbon Stereocenters by Additions of Substituted Cyanoacetate Esters to Acetylenic Esters. *Chem. Eur. J.* **2020**, 26, 10230–10239.

(15) Kabes, C. Q.; Lucas, R. F.; Gunn, J. H. Gladysz, J. A. Chiral Cobalt(III) Tris(1,2-diamine) Catalysts That Incorporate Nitrogenous Base Containing Anions for the Bifunctional Activation of Nucleophiles and Electrophiles in Enantioselective Addition Reactions. *ACS Catalysis* **2021**, *11*, 7762–7771.

(16) As of the submission date of this thesis, the best prices are (*R*,*R*)-dpen, $275/100 g and (*S*,*S*)-dpen, $271/100 g (https:// www.ambeed.com, accessed 29 May 2022).

(17) Ghosh, S. K.; Ganzmann, C.; Bhuvanesh, N.; Gladysz, J. A. Werner Complexes with

ω-Dimethylaminoalkyl Substituted Ethylenediamine Ligands: Bifunctional Hydrogen Bond Donor Catalysts for Highly Enantioselective Michael Additions. *Angew. Chem., Int. Ed.* **2016**, *55*, 4356–4360.; Werner-Komplexe mit ω-dimethylaminoalkylsubstitutierten Ethylenediamin-liganden: Bifunktionale Wasserstoffbrückenbindungsdonor-Katalysatoren für hochgradig enantioselektive Michael Additionen. *Angew. Chem.* **2016**, *128*, 4429–4433.

(18) Maximuck, W. J.; Gladysz, J. A. Lipophilic chiral cobalt (III) complexes of hexaamine ligands: Efficacies as enantioselective hydrogen bond donor catalysts. *Mol. Catal.* **2019**, *473*, 110360 (article number).

(19) (a) *Lange's Handbook of Chemistry*, 17th ed, Speight, J. G., Editor. McGraw Hill; New York, 2017, Table 2.59. (b) Any pK_a(BH^+) values not specified in the preceding reference were taken from SciFinder®, which gives predicted acidities for a number of compounds.

(20) Enantiopure chiral counter anions can exert a significant influence: Kabes, C. Q.; Maximuck, W. J.; Ghosh, S. K.; Kumar, A.; Bhuvanesh, N.; Gladysz, J. A. Chiral Tricationic Tris(1,2-diphenylethylenediamine) Cobalt(III) Hydrogen Bond Donor Catalysts with Defined Carbon/Metal Configurations; Matched/Mismatched Effects upon Enantioselectivities with Enantiomeric Chiral Counter Anions. *ACS Catal.* **2020**, *10*, 3249–3263.

(21) Some have noted the possible tribochemical role of the insoluble catalyst in this reaction. See Michalchuk, A. A. L.; Boldyreva, E. V.; Belenguer, A. M. Emmerling, F.; Boldyrev, V. V. Tribochemistry, Mechanical Alloying, Mechanochemistry. What is in a Name? *Front. Chem.* **2021**, *9*, 685789. DOI: 10.3389/fchem.2021.685789.

(22) Wititsuwannakul, T.; Hall, M. B.; Gladysz, J. A. A computational study of hydrogen bonding motifs in halide, tetrafluoroborate, hexafluorophosphate, and tetraarylborate salts of chiral cationic ruthenium and cobalt guanidinobenzimidazole hydrogen bond donor catalysts; acceptor properties of the 'BAr_f' anion. *Polyhedron* **2020**, *187*, 114618.

(23) Schmidt, R.; Scholze, H. M.; Stolle, A. Temperature progression in a mixer ball mill. *Int. J. Ind. Chem.* **2016**, *7*, 181–186.

(24) Wang, Y-F.; Chen, R-X.; Wang, K.; Zhang, B-B.; Li, Z-B.; Xu, D-Q. Fast, solvent-

free and hydrogen-bonding-mediated asymmetric Michael addition in a ball mill. *Green Chem*. **2012**, *14*, 893–895.

(25) Chauhan, P.; Chimni, S. S. Grinding-Assisted Asymmetric Organocatalysis: A Solvent-free Approach to the Formation of Vicinal Quaternary and Tertiary Stereocenters. *Asian J. Org. Chem*. **2012**, *1*, 138–141.

(26) (a) Jörres, M.; Mersmann, S.; Raabe, G.; Bolm, C. Organocatalytic solvent-free hydrogen bonding-mediated asymmetric Michael additions under ball milling conditions. *Green Chem*. **2013**, *15*, 612–616. (b) Ignatiuk, Ż. A.; Janicki, M. J.; Góra, R. W.; Konieczny, K.; Kowalczyk, R. Applications of Thermal Activation, Ball-milling and Aqueous Medium in Stereoselective Michael Addition of Nitromethane to Enynones Catalyzed by Chiral Squaramides. *Adv. Synth. Catal*. **2019**, *361*, 1108–1116.

(27) (a) Savel´yeva, T. F.; Khromova, O. V.; Larionov, V. A.; Smol´yakov, A. F.; Fedyanin, I. V.; Belokon, Y. N.; Maleev, V. I. Expanding the Family of Octahedral Chiral-at-Metal Cobalt(III) Catalysts by Introducing Tertiary Amine Moiety into the Ligand. *Catalysts* **2021**, *11*, 152 (article number). (b) Emelyanov, M. A.; Stoletova, N. V.; Lisov, A. A.; Medvedev, M. G.; Smol'yakov, A. F.; Maleev, V. I.; Larionov, V. A. An octahedral cobalt(III) complex based on cheap 1,2-phenylenediamine as a bifunctional metal-templated hydrogen bond donor catalyst for fixation of CO_2 with epoxides under ambient conditions. *Inorg. Chem. Frontiers* **2021**, *8*, 3871–3884.

(28) Ghosh, S. K.; Lewis, K. G.; Kumar, A.; Gladysz, J. A.; Syntheses of Families of Enantiopure and Diastereopure Cobalt Catalysts Derived from Trications of the Formula $[Co(NH_2)\text{-}CHArCHArNH_2)_3]^{3+}$. *Inorg. Chem*. **2017**, *56*, 2304–2320.

(29) Ishitani, H.; Kanai, K.; Yoo, W-J.; Yoshida, T.; Kobayashi, S.; A Nickel-Diamine Mesoporous Silica Composite as a Heterogeneous Chiral Catalyst for Asymmetric 1,4-Addition Reactions. *Angew. Chem. Int. Ed*. **2019**, *58*, 13313–13317.; A Nickel-Diamine/Mesoporous Silica Composite as a Heterogeneous Chiral Catalyst for Asymmetric 1,4-Addition Reactions. *Angew. Chem*. **2019**, *131*, 13447–13451.

(30) Ros Ñíguez, D.; Guillena, G.; Alonso, D.A.; Chiral 2-Aminobenzimidazoles in Deep Eutectic Mixtures: Recyclable Organocatalysts for the Enantioselective Michael Addition of 1,3-Dicarbonyl Compounds to β-Nitroalkenes. *ACS Sustainable Chem. Eng.* **2017**, *5*, 10649−10656.

3 INVESTIGATION OF ANION-CATION INTERACTIONS IN WERNER SALTS

3.1 Introduction

Upon recent years, the Werner complexes have shown to act as top-notch players in catalysis.[1] Strangely enough, the complex itself is substitution inert in its low spin d^6 electron configuration, straying from the expected catalytic characteristics.[2] While it is known that the secondary coordination sphere is where the catalytic action occurs, the exact mechanism is unknown. Within this secondary coordination sphere, the 12 NH sites hydrogen-bond to the anions, as seen in the crystal structure of $\mathbf{2}^{3+}$ $3Cl^-$ found in Figure 3.1. Single-crystal structure analysis is an advantageous route for determining reaction pathways but falls short when they are unable to crystallize well. This method also assumes the major species is similar in crystallized form as in solution. [3]

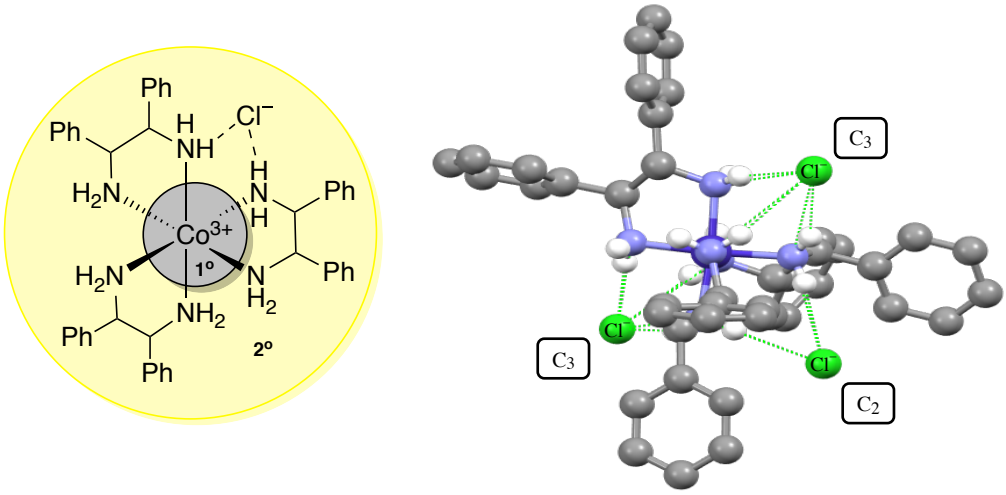

Figure 3.1. Left: The 1° and 2° coordination sphere of Λ-(*S*,*S*)-$\mathbf{2}^{3+}$ $3Cl^-$. Right: Crystal structure of Λ-(*S*,*S*)-$\mathbf{2}^{3+}$ $3Cl^-$ with hydrogen-bonding on both C_3 and C_2 faces.

Alterations in the compound's symmetry play an important role with regards to enantioselectivity, granting even greater stereoselectivity with the addition of the dpen modulated diastereomers.[4] This is an important hinderance as the yields and enantioselectivities are also dependent on the anions present in solution. To better understand this occurrence, alternate methods of observing the mechanistic behavior of the catalysts would be beneficial. One

application of such data would be to use mass spectrometry to identify certain types of "tight ion pairs" with varying trication/anion binding strengths.

Mass spectrometry has various methods to identify and quantify compounds under analysis. Techniques such as electron impact ionization (EI), a hard ionization technique, and electrospray ionization (ESI), a soft ionization technique, are a couple of the most common methods used today.[5] For analysis of the anion binding properties within the Werner complexes, the latter is expected to produce spectra with the least amount of fragmentation due to its milder conditions. This enhanced sensitivity is especially important for larger molecules (>500 kDa) to be analyzed, those of which are expected to be severely fragmented under harsh conditions. The one downside to note would be the heat applied during aerosol formation.

To better understand the catalytic mechanism of these complexes, it would be advantageous to begin with the hydrogen-bond lengths, and thus strengths, of the anions with the NH groups on the en/dpen backbone. While no computational data has been reported for the hydrogen bond strengths/lengths of the $\mathbf{2}^{3+}$ complexes, data has been compiled on similar structures to that of both $\mathbf{1}^{3+}$ and $\mathbf{2}^{3+}$. One report from our group discusses the hydrogen bond lengths for the ruthenium and cobalt complexes with the six-membered chelate, 2-guanidinobenzimidazole ligand (GBI).[6] A correlation can be established from previous findings where counter anions presenting as good hydrogen bond acceptors directly correspond with poor catalytic results.[7] This detail is crucial when evaluating the anions and their proposed effect on catalytic success.

Contrasts can be seen between Cl^-, a highly renowned hydrogen bond acceptor, and BAr_f^-, a very poor hydrogen bond acceptor, in that the former was reported to be catalytically unreactive and the latter highly reactive.[8,9] Using the ruthenium derivative of this complex, the hydrogen bond strengths were calculated and suggest hydrogen bond strengths in the following order: $F^- > Cl^- > Br^- > BF_4^- > I^- > PF_6^- > BAr_f^-$.[6] This order mirrors those calculated for the cobalt complex, both similar in series for halogen hydrogen-bonding found in literature.[9] While these complexes are not synonymous with the Werner complex under analysis in this report, some computational

results can be used as a guide for investigating catalytic success with various anions. This bond strength order inversely correlates to catalytic activity of the GBI complex, with the catalytic activity series: $Cl^- < BF_4^- < PF_6^- < BAr_f^-$.[6] Upon analyzing these series, it is proposed that the investigation of how the anions "fly" with $\mathbf{2}^{3+}$ complexes via ESI-MS could give further insight on the differences between each cation-anion interaction.

3.2. Results

In this study, observed peaks that identify with the monoisotopic mass and isotopic distribution of various combinations of the intact cation and anions were primarily investigated. "Intact", in this case, refers to species that contain the cation in its mostly unaltered form. The degradation of the catalyst post-ionization was not explored as this lies outside the scope of this study. The greatest intensity and highest m/z ratio were noted for each salt under analysis. As the intensity (%) of the peak increases, the concentration of the featured fragment proportionally increases, thus the most ionizable cation-anion matches detected post-ionization can be identified. Further analysis includes the identification of minimally fragmented components of the complexes, as the main emphasis of this project entails the cation-anion interactions. Thus, the term "unknown" may be used in place of species that do not follow these guidelines.

The first compound analyzed was Λ-(*S*,*S*)-$\mathbf{2}^{3+}$ $3Cl^-$ (Sample 1)[11] resulting in a plethora of spectral peaks, most of which were determined to be degradation of the salt (All spectra are found in Appendix B). The most intense peak (I = 100%) sits at a m/z of $[M]^+ = 553.13$ ($z = 1$), as summarized in Table 3.1. This has been identified as $[Co(dpen)_2]^{3+}$ $2Cl^-$, exhibiting the loss of one Cl^- alongside the removal of a dpen ligand. Further analysis shows the presence of $\mathbf{2}^{3+}$ $2Cl^-$ at a m/z of $[M]^+ = 765.26$ ($z = 1$) with a low intensity (11.31%), similarly losing one Cl^-. The exact ionization patterns for $\mathbf{2}^{3+}$ $2Cl^-$ and $[Co(dpen)_2]^{3+}$ $2Cl^-$ can be seen in Appendix B. The removal of two Cl^- anions alongside one hydrogen, $[Co(dpen)_3]^{3+}$ Cl^- ($-H^+$), is identified with a minimal intensity (5.73%) at $[M]^+ = 729.29$ ($z = 1$). The peak with the highest m/z ratio sits at $[M]^+ = 1568.56$ ($z = 1$), but is greater in mass than the starting compound (856.21 g/mol) with minimal intensity (0.06 %), therefore is unidentified. Various other species were identified and noted in

Table 3.1, many of which contain an unexpected anionic species (OAc^-) in the considerably pure aliquot analyzed. Species containing the OAc^- anion vary from m/z = 577.18–813.35 and all have unremarkable intensities (I < 12%). A duplicate sample of Λ-(*S*,*S*)-$\mathbf{2}^{3+}$ $3Cl^-$ (Sample 2) with an alternate method of purification including a Dowex column was analyzed for comparison. Upon advanced purification, all identified OAc^- anions were removed, leaving the same Cl^- containing species at similar intensities, seen in Table 3.1.

Table 3.1. The ESI-MS data for Λ-(*S*,*S*)-$\mathbf{2}^{3+}$ $3Cl^-$ in duplicate (Samples 1 & 2).[11]

Cation	Observed $[M]^+$ (Calculated $[M]^+$)	z	I (%)	Comment
Sample 1				
$[Co(dpen)_2]^{3+}$ $2Cl^-$	553.13 (553.13)	+1	100	**Most Intense**
$[Co(dpen)_2]^{3+}$ Cl^-OAc^-	577.18 (577.18)	+1	2.63	
$[Co(dpen)_2]^{3+}$ $2OAc^-$	601.22 (601.22)	+1	4.92	
$[Co(dpen)_3]^{3+}$ Cl^- $(-H^+)$	729.29 (729.29)	+1	5.73	Loss of a H^+
$[Co(dpen)_3]^{3+}$ $2Cl^-$	765.26 (765.26)	+1	11.31	
$[Co(dpen)_3]^{3+}$ Cl^-OAc^-	789.31 (789.31)	+1	2.06	
$[Co(dpen)_3]^{3+}$ $2OAc^-$	813.35 (813.35)	+1	1.80	
Unknown	1568.56	+1	0.06	**Greatest m/z**
Sample 2				
$[Co(dpen)_2]^{3+}$ $2Cl^-$	553.13 (553.13)	+1	100	**Most Intense**
$[Co(dpen)_3]^{3+}$ Cl^- $(-H^+)$	729.29 (729.29)	+1	5.67	Loss of a H^+
$[Co(dpen)_3]^{3+}$ $2Cl^-$	765.26 (765.26)	+1	28.20	
Unknown	1567.48	+1	0.21	**Greatest m/z**

Using the same methods, Λ-(*S*,*S*)-$\mathbf{2}^{3+}$ $2Cl^-BAr_f^-$ (Sample 3)[11] was analyzed by ESI-MS, which is summarized in Table 3.2. The most intense peak sits at m/z of $[M]^+$ = 415.18 (z = 1), identified as $\mathbf{1}^{3+}$ $3OAc^-$, displaying the loss of all six phenyl rings on the en backbone and a hydrogen atom. Upon analysis of the greatest m/z peak, $\mathbf{2}^{3+}$ $Cl^-BAr_f^-$ was identified at m/z of $[M]^+$ = 1593.36 (z = 1), where the loss of a Cl^- mirrors that of the previous sample ($\mathbf{2}^{3+}$ $3Cl^-$). The loss of both Cl^- anions and a hydrogen, $[Co(dpen)_3]^{3+}$ BAr_f^- $(-H^+)$, provides the peak at $[M]^+$ = 1557.38 (z = 1). Another interesting observation paralleling the results from the ESI-MS of $\mathbf{2}^{3+}$

$3Cl^-$ is a peak at m/z of $[M]^+$ = 553.13 (z = 1; I = 29.82) seen with the loss of a dpen ligand and a Cl^- anion. In a similar fashion, a duplicate sample (Sample 4) synthesized from Λ-(*S*,*S*)-$\mathbf{2}^{3+}$ $3Cl^-$ post-Dowex column (Sample 2) was analyzed by ESI-MS, displaying the absence of most OAc^- anions. This can be seen in the bottom of Table 3.2.

Table 3.2. The ESI-MS data for Λ-(*S*,*S*)-$\mathbf{2}^{3+}$ $2Cl^-BAr_f^-$ (Samples 3 & 4).[11]

Cation	Observed $[M]^+$ (Calculated $[M]^+$)	z	I (%)	Comment
Sample 3				
$[Co(en)_3]^{3+}$ $3OAc^-$ ($-H^+$)	415.18 (416.18)	+1	100	**Most Intense**; loss of H^+
$[Co(dpen)_2]^{3+}$ $2Cl^-$	553.13 (553.13)	+1	29.82	
$[Co(dpen)_2]^{3+}$ Cl^-OAc^-	577.18 (577.18)	+1	7.47	
$[Co(dpen)_2]^{3+}$ $2OAc^-$	601.22 (601.22)	+1	9.48	
$[Co(dpen)_3]^{3+}$ $2Cl^-$	765.27 (765.26)	+1	7.24	
$[Co(dpen)_3]^{3+}$ Cl^-OAc^-	789.31 (789.31)	+1	1.19	
$[Co(dpen)_3]^{3+}$ $2OAc^-$	813.36 (813.35)	+1	3.57	
$[Co(dpen)_3]^{3+}$ BAr_f^- ($-H^+$)	1557.38 (1557.38)	+1	0.89	Loss of H+
$[Co(dpen)_3]^{3+}$ $Cl^-BAr_f^-$	1593.36 (1593.36)	+1	0.45	**Greatest m/*z***
Sample 4				
Unknown	483.20	+1	100	**Most Intense**
$[Co(dpen)_2]^{3+}$ $2Cl^-$	553.13 (553.13)	+1	83.13	
$[Co(dpen)_2]^{3+}$ Cl^-OAc^-	577.18 (577.18)	+1	2.42	
$[Co(dpen)_3]^{3+}$ Cl^- ($-H^+$)	729.29 (729.29)	+1	5.80	Loss of H^+
$[Co(dpen)_3]^{3+}$ $2Cl^-$	765.26 (765.26)	+1	33.15	
$[Co(dpen)_3]^{3+}$ BAr_f^- ($-H^+$)	1557.37 (1557.38)	+1	0.91	Loss of H^+
$[Co(dpen)_3]^{3+}$ $Cl^-BAr_f^-$	1593.37 (1593.36)	+1	2.80	**Greatest m/z**

For comparison, the diastereomer of the previous compound, Δ-(*S*,*S*)- $\mathbf{2}^{3+}$ $2Cl^-BAr_f^-$ (Sample 5),[11] was analyzed. Very few spectral peaks were observed and even less were identified, as summarized in Table 3.3. The most intense peak as well as the greatest m/z are unidentified at a low m/z of $[M]^+$ = 149.01 (z = 1) and 1557.38 (z = 1), respectively. The only labelled species sits at a m/z of $[M]^+$ = 231.77 (z = 1) with minimal intensity (I = 0.07).

Table 3.3. The ESI-MS data for Δ-(*S*,*S*)-$\mathbf{2}^{3+}$ 2Cl$^-$BAr$_f^-$ (Sample 5).[11]

Cation	Observed $[M]^+$ (Calculated $[M]^+$)	*z*	I (%)	Comment
Unknown	149.01	+1	100	**Most Intense**
$[Co(dpen)_3]^{3+}$	231.77 (231.78)	+3	0.07	
$[Co(dpen)_3]^{3+}$ BAr$_f^-$ ($-H^+$)	1557.38 (1557.38)	+1	0.60	**Greatest m/z**

For the salt Λ-(*S*,*S*)-$\mathbf{2}^{3+}$ 3BF$_4^-$ (Sample 6),[11] the most intense peak found at a m/*z* of $[M]^+$ = 299.15 (*z* = 1) is much lower in mass than previous species identified at intensities of 100% and in this case the identity is unknown. More anionic compounds that are not seen in the salt under analysis continue to show in species with $[M]^+ > 550$, this time including both OAc$^-$ and Cl$^-$. At a m/*z* of $[M]^+$ = 299.15 (*z* = 1), the loss of one BF$_4^-$ anion, $\mathbf{2}^{3+}$ 2BF$_4^-$, is identified at minimal intensity (I < 1). Lastly, the greatest m/*z* peak is considered unknown at a m/*z* of $[M]^+$ = 1325.88 (*z* = 1).

Table 3.4. The ESI-MS data for Λ-(*S*,*S*)-$\mathbf{2}^{3+}$ 3BF$_4^-$ (Sample 6).[11]

Cation	Observed $[M]^+$ (Calculated $[M]^+$)	*z*	I (%)	Comment
Unknown	299.15	+1	100	**Most Intense**
$[Co(dpen)_2]^{3+}$ 2Cl$^-$	553.13 (553.13)	+1	15.98	
$[Co(dpen)_2]^{3+}$ Cl$^-$OAc$^-$	577.18 (577.18)	+1	4.91	
$[Co(dpen)_3]^{3+}$ BF$_4^-$ ($-H^+$)	781.32 (781.32)	+1	2.50	Loss of H^+
$[Co(dpen)_3]^{3+}$ 2OAc$^-$	813.35 (813.35)	+1	6.74	
$[Co(dpen)_3]^{3+}$ 2BF$_4^-$	869.33 (869.33)	+1	0.96	
Unknown	1325.88	+1	1.18	**Greatest m/z**

Similarly to the results of Λ-(*S*,*S*)-$\mathbf{2}^{3+}$ 3BF$_4^-$, the salt Λ-(*S*,*S*)-$\mathbf{2}^{3+}$ 3PF$_6^-$ (Sample 7)[11] contains a peak at a m/*z* of $[M]^+$ = 299.15 (*z* = 1) at the max intensity, and remains unidentified. Other mirroring results include the peaks at $[M]^+$ = 553.13 (*z* = 1) and 557.18 (*z* = 1), each with enhanced intensities. The greatest m/*z* peak is identified as Λ-(*S*,*S*)-$\mathbf{2}^{3+}$ Cl$^-$BAr$_f^-$, a considered impurity of the instrument with minimal intensity (I < 1).

Table 3.5. The ESI-MS data for Λ-(*S,S*)-$\mathbf{2}^{3+}$ $3PF_6^-$ (Sample 7).[11]

Cation	Observed $[M]^+$ (Calculated $[M]^+$)	z	I (%)	Comment
Unknown	299.15	+1	100	**Most Intense**
$[Co(dpen)_2]^{3+}$ $2Cl^-$	553.13 (553.13)	+1	58.37	
$[Co(dpen)_2]^{3+}$ Cl^-OAc^-	577.18 (577.18)	+1	2.73	
$[Co(dpen)_3]^{3+}$ $2Cl^-$	765.27 (765.26)	+1	3.81	
$[Co(dpen)_3]^{3+}$ $Cl^-BAr_f^-$	1593.36 (1593.36)	+1	0.13	**Greatest m/z**

For Λ-(*S,S*)-$\mathbf{2}^{3+}$ $Cl^-BAr_f^-Nic^-$ (Sample 8),[14] the most intense, $[M]^+ = 365.14$ ($z = 1$), and greatest m/z, $[M]^+ = 1646.39$ ($z = 1$), are unknown. The loss of both Cl^- and BAr_f^- noticed at $[M]^+ = 816.35$ ($z = 1$) as well as the loss of both Cl^- and Nic^- seen at $[M]^+ = 1557.42$ ($z = 1$) show at minimal intensity (I < 1), as summarized in Table 3.6, below.

Table 3.6. The ESI-MS data for Λ-(*S,S*)-$\mathbf{2}^{3+}$ $Cl^-BAr_f^-Nic^-$ (Sample 8).[14]

Cation	Observed $[M]^+$ (Calculated $[M]^+$)	z	I (%)	Comment
Unknown	365.14	+1	100	**Most Intense**
$[Co(dpen)_3]^{3+}$ Nic^- $(-H^+)$	816.35 (816.34)	+1	0.54	Loss of H^+
$[Co(dpen)_3]^{3+}$ BAr_f^- $(-H^+)$	1557.42 (1557.38)	+1	0.33	Loss of H^+
Unknown	1646.39	+1	0.02	**Greatest m/z**

Interestingly, Λ-(*S,S*)-$\mathbf{2}^{3+}$ $3SbF_6^-$ (Sample 9)[15] displayed $\mathbf{2}^{3+}$ $2Cl^-$ as the most abundant species post-ionization at the repeating peak $[M]^+ = 553.13$ ($z = 1$), as seen in Table 3.7. The final three salts analyzed under ESI-MS, Λ-(*S,S*)-$\mathbf{2}^{3+}$ 3(S)-camphorSO_3^- (Sample 10),[20] Λ-(*S,S*)-$\mathbf{2}^{3+}$ 3(1R)-BINOLPA$^-$ (Sample 11),[20] and Λ-(*S,S*)-$[Pt(en)_3]^{4+}$ $4BAr_f^-$ (Sample 12),[13] concluded with no identified cation-anion species post-ionization and are summarized in Tables 3.8–3.10. The most intense peaks reside at a m/z of $[M]^+ = 349.06$, 161.06, and 1315.29 ($z = 1$), respectively. The greatest m/z peaks all are minimal in intensity (I < 2%), with peaks at $[M]^+ = 1666.90$, 1666.90, and 2445.71 ($z = 1$), respectively.

Table 3.7. The ESI-MS data for Λ-(*S*,*S*)-$\mathbf{2}^{3+}$ $3SbF_6^-$ (Sample 9).[15]

Cation	Observed $[M]^+$ (Calculated $[M]^+$)		I (%)	Comment
Unknown	299.15	+1	19.38	
$[Co(dpen)_2]^{3+}$ $2Cl^-$	553.13	+1	100	**Most Intense**
Unknown	1344.57	+1	0.10	**Greatest m/z**

Table 3.8. The ESI-MS data for Λ-(*S*,*S*)-$\mathbf{2}^{3+}$ 3(S)-camphorSO_3^- (Sample 10).[20]

Cation	Observed $[M]^+$ (Calculated $[M]^+$)	z	I (%)	Comment
Unknown	349.06	+1	100	**Most Intense**
Unknown	1666.90	+1	0.28	**Greatest m/z**

Table 3.9. The ESI-MS data for Λ-(*S*,*S*)-$\mathbf{2}^{3+}$ 3(1R)-BINOLPA^- (Sample 11).[20]

Cation	Observed $[M]^+$ (Calculated $[M]^+$)	*z*	I (%)	Comment
Unknown	161.06	+1	100	**Most Intense**
Unknown	1666.90	+1	1.71	**Greatest m/z**

Table 3.10. The ESI-MS data for Λ-(*S*,*S*)-$[Pt(en)_3]^{4+}$ $4BAr_f^-$ (Sample 12).[13]

Cation	Observed $[M]^+$ (Calculated $[M]^+$)	*z*	I (%)	Comment
Unknown	1315.29	+1	100	**Most Intense**
Unknown	2445.71	+1	0.19	**Greatest m/z**

3.3 Discussion

Throughout the Werner salts analyzed under ESI-MS, few showed the anion successfully "flying" with the cation. The most promising under these conditions being Λ-(*S*,*S*)-$\mathbf{2}^{3+}$ $3Cl^-$, where both $[Co(dpen)_2]^{3+}$ $2Cl^-$ and $\mathbf{2}^{3+}$ $2Cl^-$ are observed, displaying the loss of one Cl^-. While originally three chloride ions were present, the bond strengths are largely dependent on the face in which hydrogen bonding occurs. By looking at the crystal structure seen in Figure 3.1 of $\mathbf{2}^{3+}$ $3Cl^-$, it may be inferred that one Cl^- remains on each C_3 axis face and the third on the C_2 face. The hydrogen-bonds ($Cl^{\cdots}HN$) on the C_3 axis are reasonably stronger than that of the C_2 face due to both the angle of accessibility as well as the number of vacant NH groups present.[10,11]

This phenomenon is also seen to occur with Λ-(*S*,*S*)-$\mathbf{2}^{3+}$ $2Cl^-BAr_f^-$, with the production of $\mathbf{2}^{3+}$ $Cl^-BAr_f^-$. In contradiction to the hydrogen-bond strengths listed previously as well as the formation of $\mathbf{2}^{3+}$ $Cl^-BAr_f^-$, the presence of $\mathbf{2}^{3+}$ $2Cl^-$ indicates that the BAr_f^- anion is removed prior to the Cl^- anion. This insinuates this species could be an impurity seen in the other samples tested. Another possibility is the relative concentration of the anions (Cl^-:BAr_f^- 2:1) in the sample is not consistent post-ionization. This could be due to the degradation of the larger/bulkier anion. Also seen from Λ-(*S*,*S*)-$\mathbf{2}^{3+}$ $2Cl^-BAr_f^-$ is the formulation of $\mathbf{1}^{3+}$ $3OAc^-$ ($-H^+$), noting the loss of one hydrogen from one NH group on the en ligand. This is the expected location of abstraction due to the great acidity of these hydrogens in comparison to those contained on the carbons in the en ligands ($H_2N-(C\underline{\boldsymbol{H}}_2)_2-NH_2$).

Upon purification of Λ-(*S*,*S*)-$\mathbf{2}^{3+}$ $3Cl^-$ with the additional step of a Dowex column, all identified OAc^- species were removed. This parallels with the subsequently derived Λ-(*S*,*S*)-$\mathbf{2}^{3+}$ $2Cl^-BAr_f^-$, with the exception of one OAc^- species at a low intensity of 2.42. In both cases, the increased intensity (~2.5x) of Cl^- containing species, $\mathbf{2}^{3+}$ $2Cl^-$, from the washed sample to the post-Dowex sample is noted. This indicates that typical purification methods of washing the catalysts with solvent, as opposed to the time consuming Dowex column, is not sufficient for analytical purification.

Other species identified to contain anions undetectable in the salt under analysis (i.e. OAc^- and Cl^-) are considered artifacts from previous starting materials, $Co(OAc)_2$ and $\mathbf{2}^{2+}$ $3Cl^-$, respectively.[11,12] The former is introduced as the original source for the cobalt center and the latter as the most common salt for anion metathesis to subsequent salts. Since all samples are analyzed by both ^1H and ^{13}C NMR to be relatively pure prior to use, the presence of these anions (i.e. OAc^- and Cl^-) could indicate they out-compete other anions during ionization. For this reason, these results only indicate what species are present post-ionization as opposed to in solution during catalysis. It is important to note that no matter the intensity of the observed peak, the intensity remains relative to the additional species present post-ionization. This is especially important for the most intense peak ($\mathbf{1}^{3+}$ $3OAc^-$) found in Λ-(*S*,*S*)-$\mathbf{2}^{3+}$ $2Cl^-BAr_f^-$.

In each case the greatest m/*z* is substantial in comparison to the mass of the salts. This suggests some dimerized species could be formed during ionization as well as impurities in the instrument itself.

3.4 Conclusion

To better understand the anion effect of Werner catalysts on catalysis, ESI-MS was used to observe the cation-anion interactions. Throughout the analysis of ten salts of $\mathbf{2}^{3+}$, only half showed anions "flying" with the cation: Λ -(*S*,*S*)-$\mathbf{2}^{3+}$ $2Cl^-$, Λ/Δ -(*S*,*S*)-$\mathbf{2}^{3+}$ $2Cl^-BAr_f^-$, Λ-(*S,S*)-$\mathbf{2}^{3+}$ $Cl^-BAr_f^-Nic^-$, and, Λ -(*S*,*S*)-$\mathbf{2}^{3+}$ $3BF_4^-$. The first two displayed the loss of one–two Cl^- anions with the third and fourth also displaying the loss of one BAr_f^- anion. The Nic^- containing salt further displayed the loss of Nic^- and the BF_4^- containing salt resulted with the loss of one–two BF_4^- anions. While impurities were found in most cases, the larger, bulkier anions seemed to be degraded themselves leaving no indication of intact cation-anion species post-ionization. From duplicate samples, it seems purification techniques should be taken seriously with regards to removing the unwanted anions.

3.5 Experimental

These experiments were performed using a Thermo Scientific Q Exactive Focus. The sample was loop injected (10 μL) and methanol was used as a mobile phase at a flow rate of 600 μL/min. The Q Exactive Focus HESI source was operated in full MS in positive mode. The mass resolution was tuned to 70000 FWHM at m/*z* 200. The spray voltage was set to 3.5 kV for positive mode and 2.8 kV for negative mode. The sheath gas and auxiliary gas flow rates were set to 30 and 0 arbitrary units, respectively. The transfer capillary temperature was held at 270 °C and the S-Lens RF level was set at 50 v. Exactive Series 2.11 /Xcalibur 4.2.47 software was used for data acquisition and processing.

3.6 References

(1) Lewis, K. G.; Ghosh, S. K.; Bhuvanesh, N.; Gladysz, J. A. Cobalt(III) Werner Complexes with 1,2-Diphenylethylenediamine Ligands: Readily Available, Inexpensive, and

Modular Chiral Hydrogen Bond Donor Catalysts for Enantioselective Organic Synthesis. *ACS Cent. Sci.* **2015**, *1*, 5–56.

(2) Ehnbom, A.; Ghosh, S. K.; Lewis, K. G.; Gladysz, J. A. Octahedral Werner complexes with substituted ethylenediamine ligands: a stereochemical primer for a historic series of compounds now emerging as a modern family of catalysts. *Chem. Soc. Rev.* **2016**, *45*, 6799–6811.

(3) Evans, C.; Mackay, K. M.; Nicholson, B. K. The formation of mixed germanium–cobalt carbonyl clusters: an electrospray mass spectrometric study, and the structure of a high-nuclearity $[Ge_2Co_{10}(CO)_{24}]^{2-}$ anion. *J. Chem. Soc., Dalton Trans.* **2001**, 1645–1649.

(4) Lewis, K. G.; Ghosh, S. K.; Bhuvanesh, N.; Gladysz, J. A. Cobalt(III) Werner Complexes with 1,2-Diphenylethylenediamine Ligands: Readily Available, Inexpensive, and Modular Chiral Hydrogen Bond Donor Catalysts for Enantioselective Organic Synthesis. *ACS Cent. Sci.* **2015**, *1*, 50–56.

(5) Jirásko, R.; Holčapek, M. Structural analysis of organometallic compounds with soft ionization mass spectrometry. *Mass Spectrom. Rev.* **2011**, *30*, 1013–1036.

(6) Wititsuwannakul, T.; Hall, M. B.; Gladysz, J. A. A computational study of hydrogen bonding motifs in halide, tetrafluoroborate, hexafluorophosphate, and tetraarylborate salts of chiral cationic ruthenium and cobalt guanidinobenzimidazole hydrogen bond donor catalysts; acceptor properties of the "BAr_f" anion. *Polyhedron* **2020**, *187*, 114618.

(7) (a) Scherer, A.; Mukherjee, T.; Hampel, F.; Gladysz, J. A. Metal-Templated Hydrogen Bond Donors as "Organocatalysts" for Carbon–Carbon Bond Forming Reactions: Syntheses, Structures, and Reactivities of 2-Guanidinobenzimidazole Cyclopentadienyl Ruthenium Complexes. *Organometallics* **2014**, *33*, 6709–6722. (b) Mukherjee, T.; Ganzmann, C.; Bhuvanesh, N.; Gladysz, J. A. Syntheses of Enantiopure Bifunctional 2-Guanidinobenzimidazole Cyclopentadienyl Ruthenium Complexes: Highly Enantioselective Organometallic Hydrogen Bond Donor Catalysts for Carbon–Carbon Bond Forming Reactions. *Organometallics* **2014**, *33*, 6723–6737. (c) Mukherjee, T.; Ghosh, S. K.; Wititsuwannakul, T.; Bhuvanesh, N.; Gladysz, J. A. Chiral-at-Metal Ruthenium Complexes with Guanidinobenzimidazole and

Pentaphenylcyclopentadienyl Ligands: Synthesis, Resolution, and Preliminary Screening as Enantioselective Second Coordination Sphere Hydrogen Bond Donor Catalysts. *Organometallics* **2020**, *39*, 1163–1175.

(8) (a) Cláudio, A. F. M.; Swift, L.; Hallett, J. P.; Welton, T.; Coutinho, J. A. P.; Freire, M. G. Extended scale for the hydrogen-bond basicity of ionic liquids. *Phys. Chem. Chem. Phys.* **2014**, *16*, 6593. (b) Lungwitz, R.; Spange, S. A hydrogen bond accepting (HBA) scale for anions, including room temperature ionic liquids. *New J. Chem.* **2008**, *32*, 392. (c) Pike, S. J.; Hutchinson, J. J.; Hunter, C. A. H-Bond Acceptor Parameters for Anions. *J. Am. Chem. Soc.* **2017**, *139*, 6700–6706.

(9) Kovacs, A.; Varga, Z. Halogen acceptors in hydrogen bonding. *Coord. Chem. Rev.* **2006**, *250*, 710–727.

(10) Luu, Q. H.; Lewis, K. G.; Banerjee, A.; Bhuvanesh, N.; Gladysz, J. A. The Robust, Readily Available Cobalt(III) Trication $[Co(NH_2CHPhCHPhNH_2)_3]^{3+}$ is a Progenitor of Broadly Applicable Chirality and Prochirality Sensing Agents. *Chem. Sci.* **2018**, *9*, 5087–5099.

(11) Ghosh, S. K.; Lewis, K. G.; Kumar, A.; Gladysz, J. A. Syntheses of Families of Enantiopure and Diastereopure Cobalt Catalysts Derived from Trications of the Formula $[Co(NH_2CHPhCHPhNH_2)_3]^{3+}$. *Inorg. Chem.* **2017**, *56*, 2304–2320.

(12) Wegener, A. R.; Kabes, C. Q.; Gladysz, J. A. Launching Werner Complexes into the Modern Era of Catalytic Enantioselective Organic Synthesis. *Acc. Chem. Res.* **2020**, *53*, 2299–2313.

(13) Maximuck, W. J.; Ganzmann, C.; Alvi, S.; Hooda, K. R.; Gladysz, J. A. Rendering classical hydrophilic enantiopure Werner salts $[M(en)_3]^{n+}$ nX^- lipophilic (M/n = Cr/3, Co/3, Rh/3, Ir/3, Pt/4); new chiral hydrogen bond donor catalysts and enantioselectivities as a function of metal and charge. *Dalton Trans.* **2020**, *49*, 3680–3691.

(14) Kabes, Connor Q.; Lucas, Reagan F.; Gunn, Jack H.; Gladysz, John A. Chiral Cobalt(III) Tris(1,2-diamine) Catalysts That Incorporate Nitrogenous Base Containing Anions for

the Bifunctional Activation of Nucleophiles and Electrophiles in Enantioselective Addition Reactions. *ACS Catal*. **2021**, 11, 7762–7771.

(15) Maximuck, William Joseph. *Syntheses of Lipophilic Werner Complexes for Application as Chiral Hydrogen Bond Donors in Enantioselective Catalysis and Investigation of the Effect of Chloride on Fluid Catalytic Cracking Catalysis*: Texas A&M University, 2021.

(20) Enantiopure chiral counter anions can exert a significant influence: Kabes, C. Q.; Maximuck, W. J.; Ghosh, S. K.; Kumar, A.; Bhuvanesh, N.; Gladysz, J. A. Chiral Tricationic Tris(1,2-diphenylethylenediamine) Cobalt(III) Hydrogen Bond Donor Catalysts with Defined Carbon/Metal Configurations; Matched/Mismatched Effects upon Enantioselectivities with Enantiomeric Chiral Counter Anions. *ACS Catal*. **2020**, *10*, 3249–3263.

APPENDIX A: HPLC TRACES FOR ENANTIOSELECTIVE NTROOLEFIN ADDITION REACTIONS USING BIFUNCTIONAL ANIONS AND A BALL MILL

Dimethyl 2-(2-nitro-1-phenylethyl)malonate (6a)

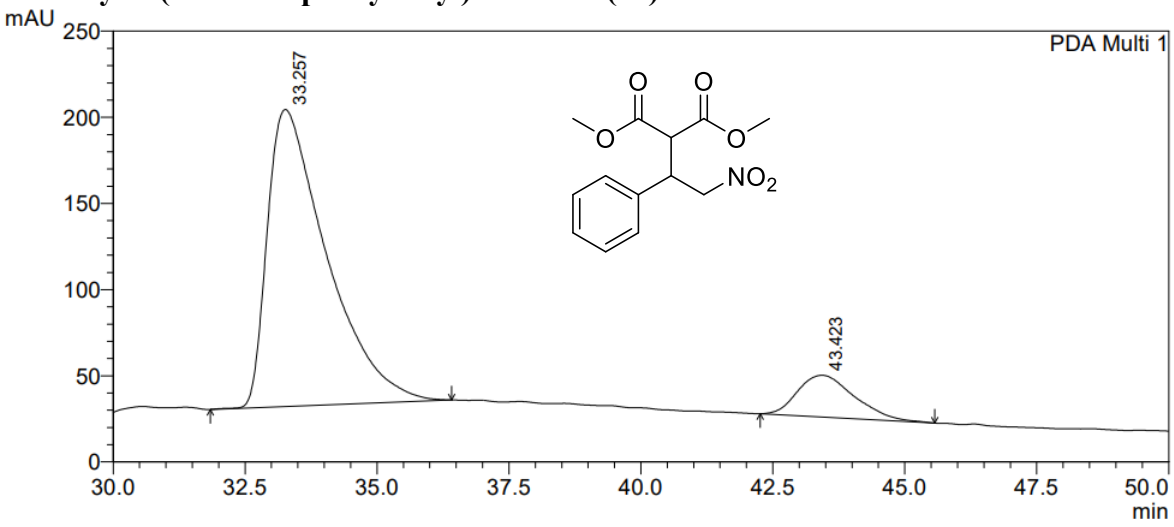

1 PDA Multi 1/220nm 4nm

PeakTable

PDA Ch1 220nm 4nm

Peak#	Ret. Time	Area	Height	Area %	Height %
1	33.257	13519347	172357	88.096	87.676
2	43.423	1826888	24227	11.904	12.324
Total		15346235	196584	100.000	100.000

Diethyl 2-(2-nitro-1-phenylethyl)malonate (6a−Et)

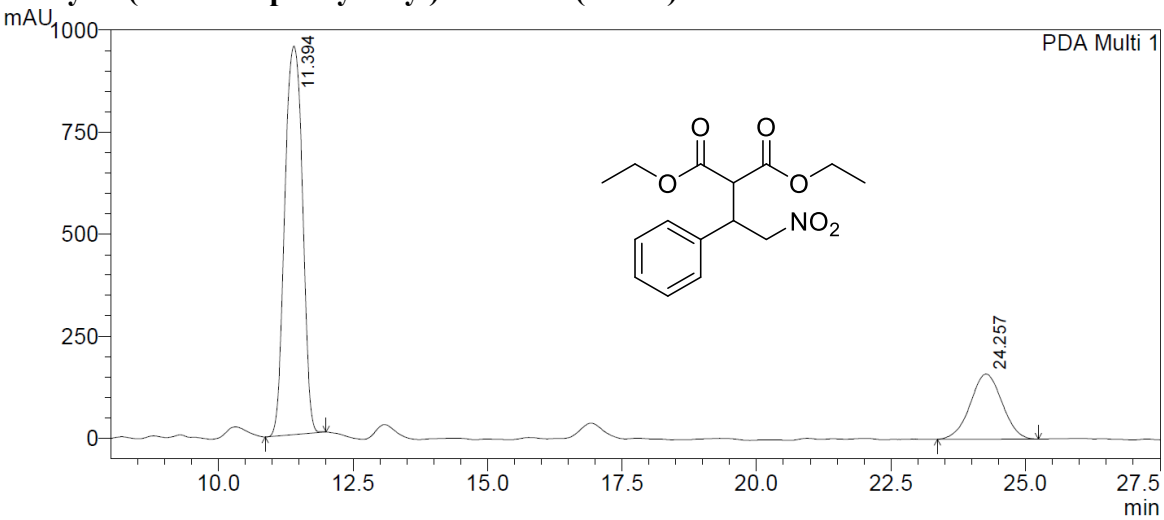

1 PDA Multi 1/220nm 4nm

PeakTable

PDA Ch1 220nm 4nm

Peak#	Ret. Time	Area	Height	Area %	Height %
1	11.394	21853017	952644	76.846	85.639
2	24.257	6584265	159752	23.154	14.361
Total		28437282	1112396	100.000	100.000

Dimethyl 2-(2-nitro-1-(4-methoxyphenyl)ethyl)malonate (6b)

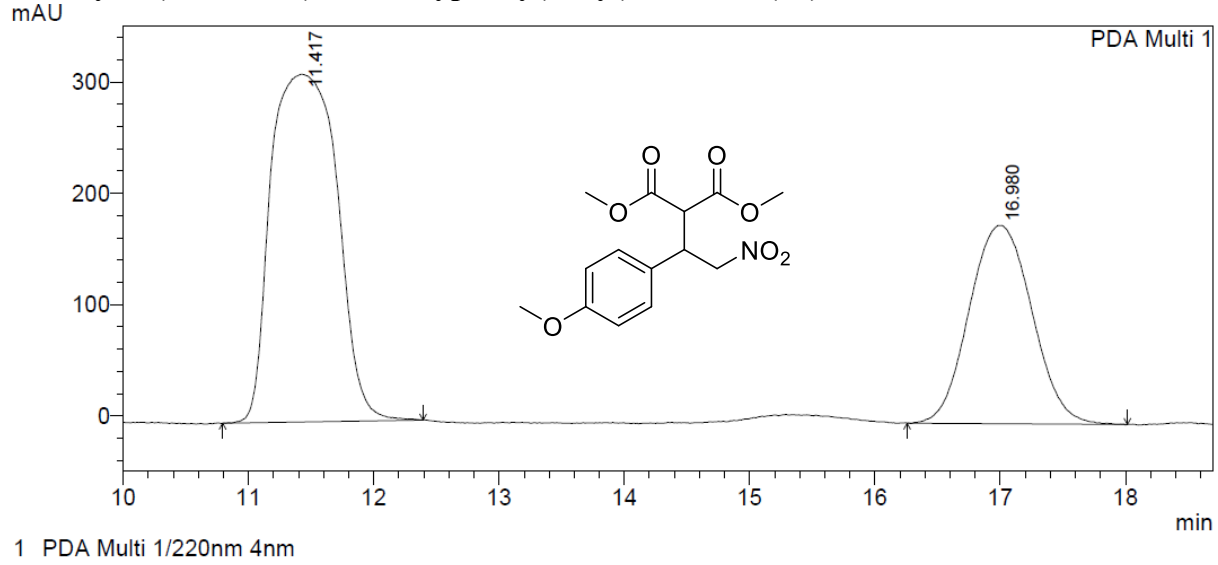

1 PDA Multi 1/220nm 4nm

PeakTable

PDA Ch1 220nm 4nm

Peak#	Ret. Time	Area	Height	Area %	Height %
1	11.417	11525146	312474	65.037	63.696
2	16.980	6195760	178097	34.963	36.304
Total		17720905	490571	100.000	100.000

Dimethyl 2-(2-nitro-1-(4-nitrophenyl)ethyl)malonate (6c)

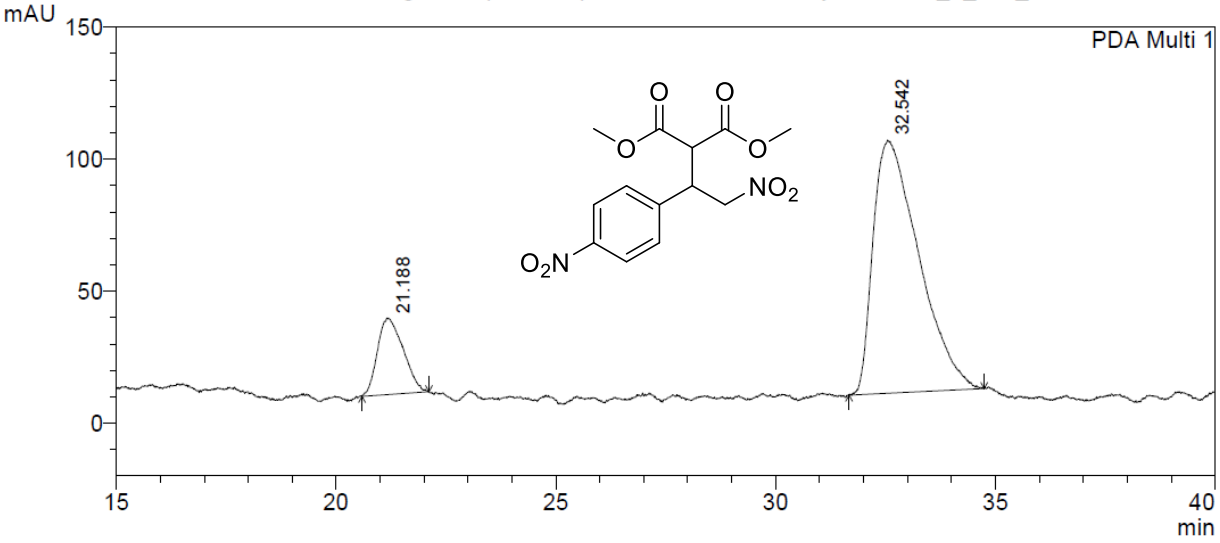

1 PDA Multi 1/220nm 4nm

PeakTable

PDA Ch1 220nm 4nm

Peak#	Ret. Time	Area	Height	Area %	Height %
1	21.188	1183256	28983	14.625	23.201
2	32.542	6907273	95940	85.375	76.799
Total		8090528	124922	100.000	100.000

Dimethyl 2-(2-nitro-1-(2-trifluoromethylphenyl)ethyl)malonate (6d)

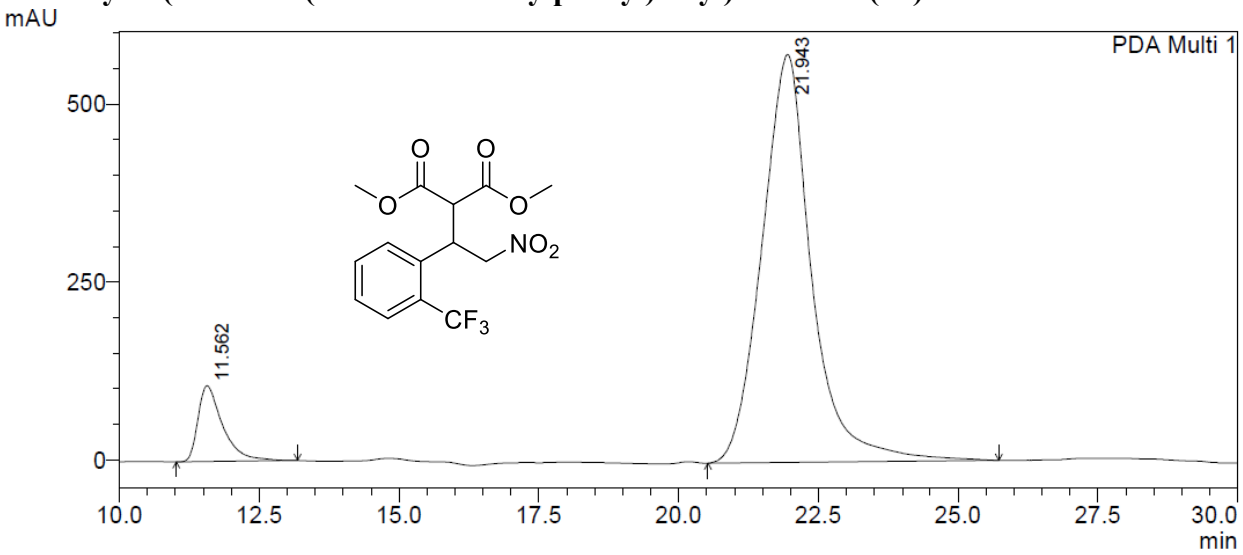

1 PDA Multi 1/220nm 4nm

PeakTable

PDA Ch1 220nm 4nm

Peak#	Ret. Time	Area	Height	Area %	Height %
1	11.562	3270481	106304	8.449	15.653
2	21.943	35437678	572828	91.551	84.347
Total		38708159	679132	100.000	100.000

Dimethyl 2-(2-nitro-1-(2-acetoxyphenyl)ethyl)malonate (6e)

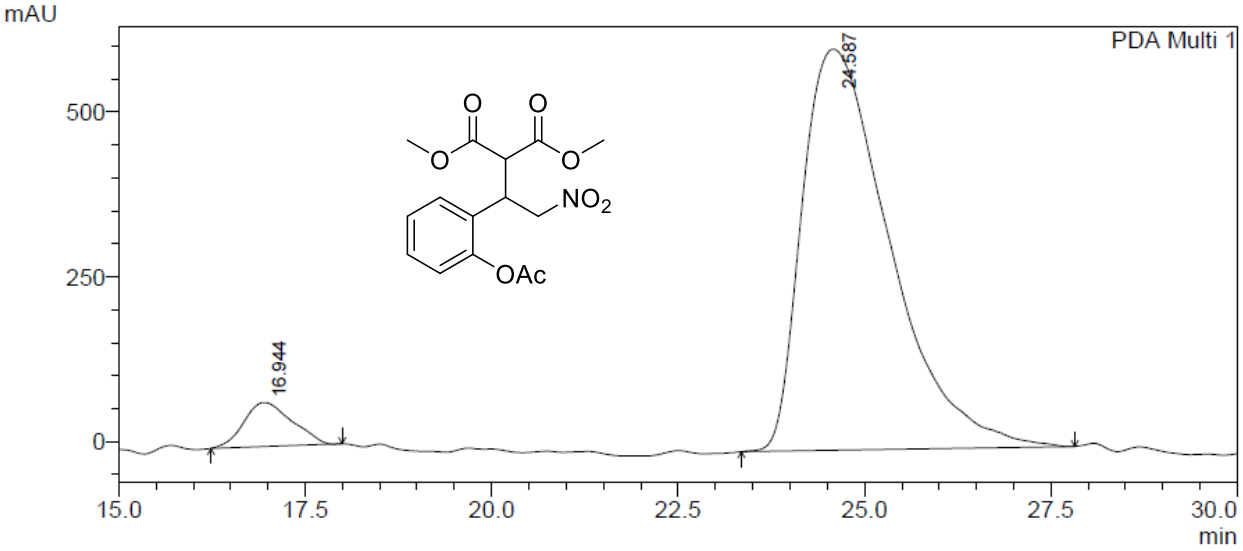

1 PDA Multi 1/220nm 4nm

PeakTable

PDA Ch1 220nm 4nm

Peak#	Ret. Time	Area	Height	Area %	Height %
1	16.944	2995425	66789	5.680	9.898
2	24.587	49742251	608004	94.320	90.102
Total		52737676	674793	100.000	100.000

Dimethyl 2-(2-nitro-1-(2-benzoyloxyphenyl)ethyl)malonate (6f)

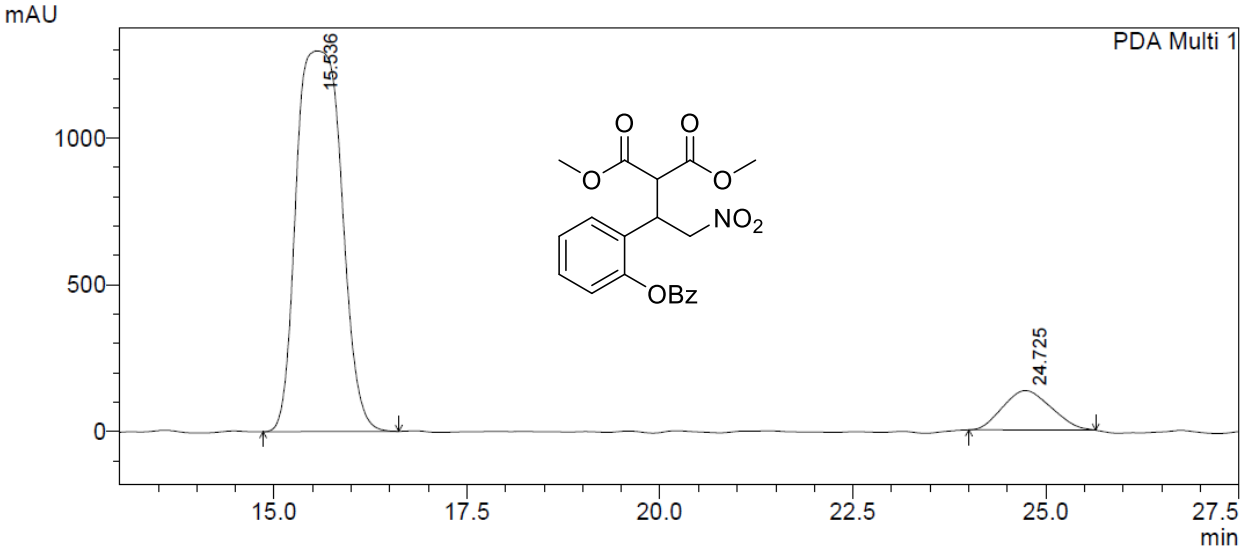

1 PDA Multi 1/220nm 4nm

PeakTable

PDA Ch1 220nm 4nm

Peak#	Ret. Time	Area	Height	Area %	Height %
1	15.536	53024789	1295423	90.042	90.591
2	24.725	5864069	134543	9.958	9.409
Total		58888858	1429967	100.000	100.000

Dimethyl 2-(2-nitro-1-(2-benzyloxyphenyl)ethyl)malonate (6g)

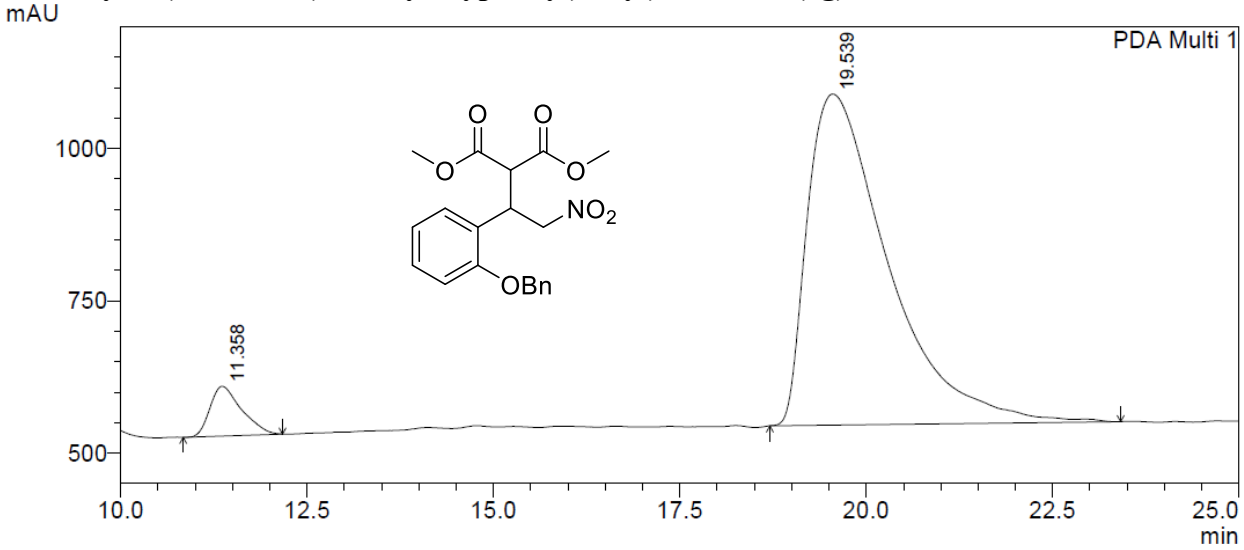

1 PDA Multi 1/220nm 4nm

PeakTable

PDA Ch1 220nm 4nm

Peak#	Ret. Time	Area	Height	Area %	Height %
1	11.358	2409993	81505	5.544	13.042
2	19.539	41064186	543419	94.456	86.958
Total		43474179	624924	100.000	100.000

Dimethyl 2-(2-nitro-1-(2-methylphenyl)ethyl)malonate (6h)

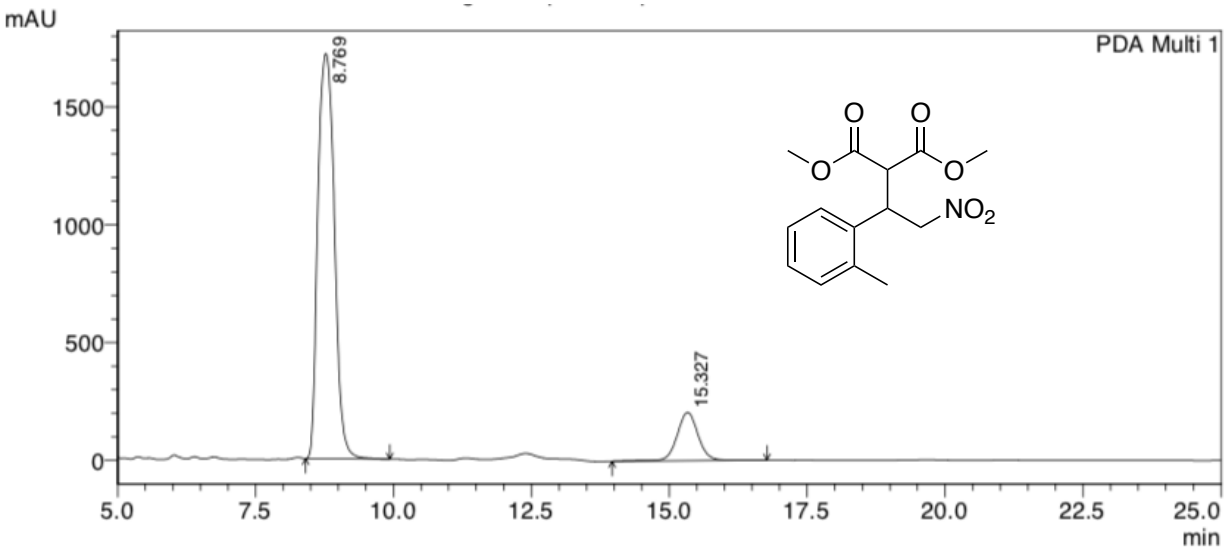

1 PDA Multi 1/220nm 4nm

PeakTable

PDA Ch1 220nm 4nm

Peak#	Ret. Time	Area	Height	Area %	Height %
1	8.769	35864370	1718684	86.813	89.352
2	15.327	5447796	204806	13.187	10.648
Total		41312166	1923490	100.000	100.000

Dimethyl 2-(2-nitro-1-β-naphthylethyl)malonate (6i)

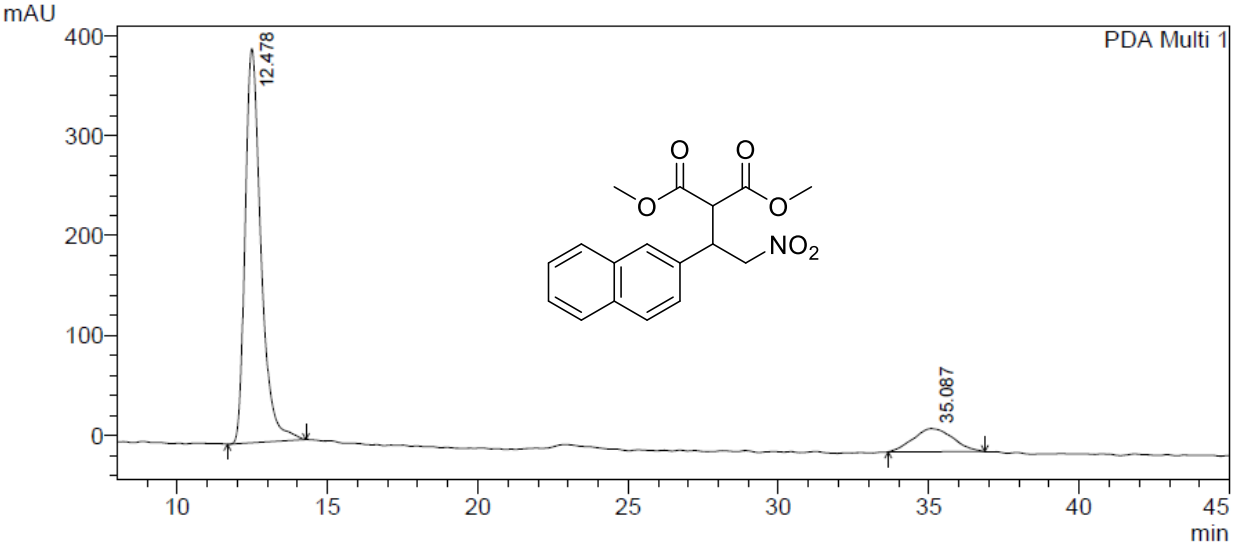

1 PDA Multi 1/254nm 4nm

PeakTable

PDA Ch1 254nm 4nm

Peak#	Ret. Time	Area	Height	Area %	Height %
1	12.478	14511741	394517	87.110	94.436
2	35.087	2147326	23246	12.890	5.564
Total		16659066	417762	100.000	100.000

Dimethyl 2-(2-nitro-1-α-naphthylethyl)malonate (6j)

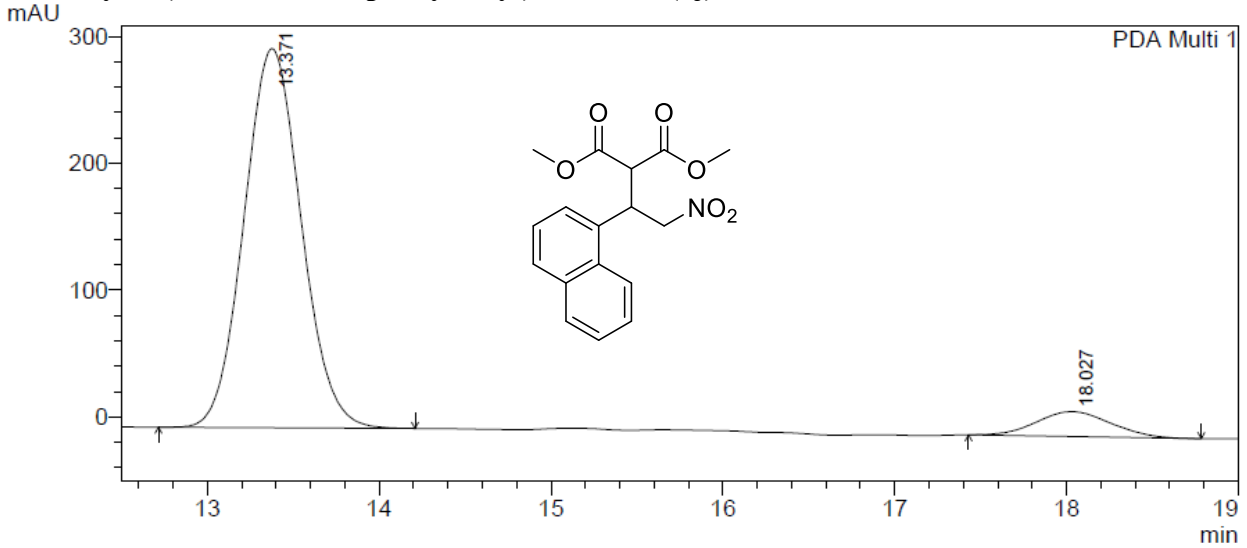

1 PDA Multi 1/254nm 4nm

PeakTable

PDA Ch1 254nm 4nm

Peak#	Ret. Time	Area	Height	Area %	Height %
1	13.371	6918008	298872	92.143	93.849
2	18.027	589928	19590	7.857	6.151
Total		7507937	318462	100.000	100.000

Dimethyl 2-(2-nitro-1-(3,4-dioxolophenyl)ethyl)malonate (6k)

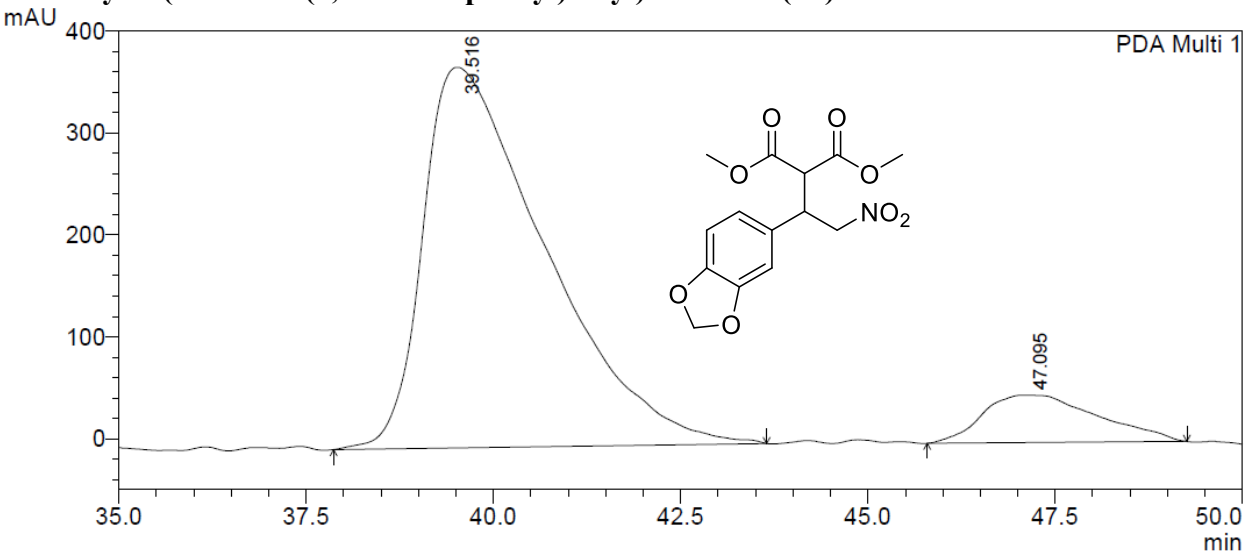

1 PDA Multi 1/220nm 4nm

PeakTable

PDA Ch1 220nm 4nm

Peak#	Ret. Time	Area	Height	Area %	Height %
1	39.516	42465786	373323	89.513	88.901
2	47.095	4974918	46607	10.487	11.099
Total		47440703	419930	100.000	100.000

Dimethyl 2-(2-nitro-1-furylethyl)malonate (6l)

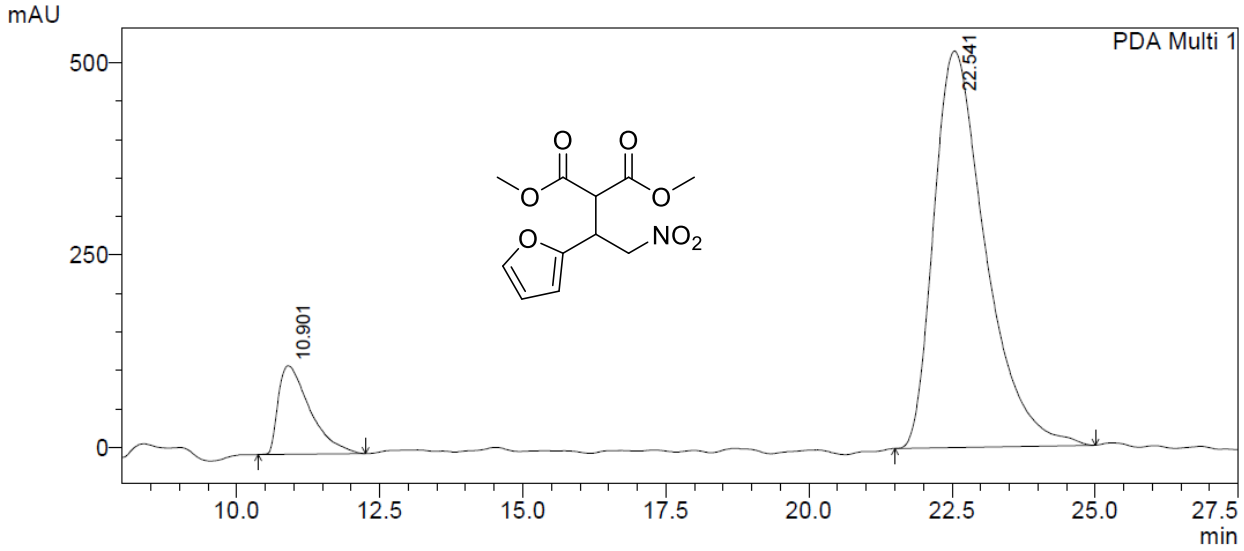

1 PDA Multi 1/220nm 4nm

PeakTable

PDA Ch1 220nm 4nm

Peak#	Ret. Time	Area	Height	Area %	Height %
1	10.901	4446916	114985	12.064	18.251
2	22.541	32415437	515026	87.936	81.749
Total		36862353	630011	100.000	100.000

APPENDIX B: ESI-MS SPECTRA FOR VARIOUS WERNER SALTS

Sample 1: Λ-(*S*,*S*)-$[Co(dpen)_3]^{3+}$ $3Cl^- \bullet 3H_2O$

Other Species Used in Synthesis: $Co(OAc)_2$; MeOH

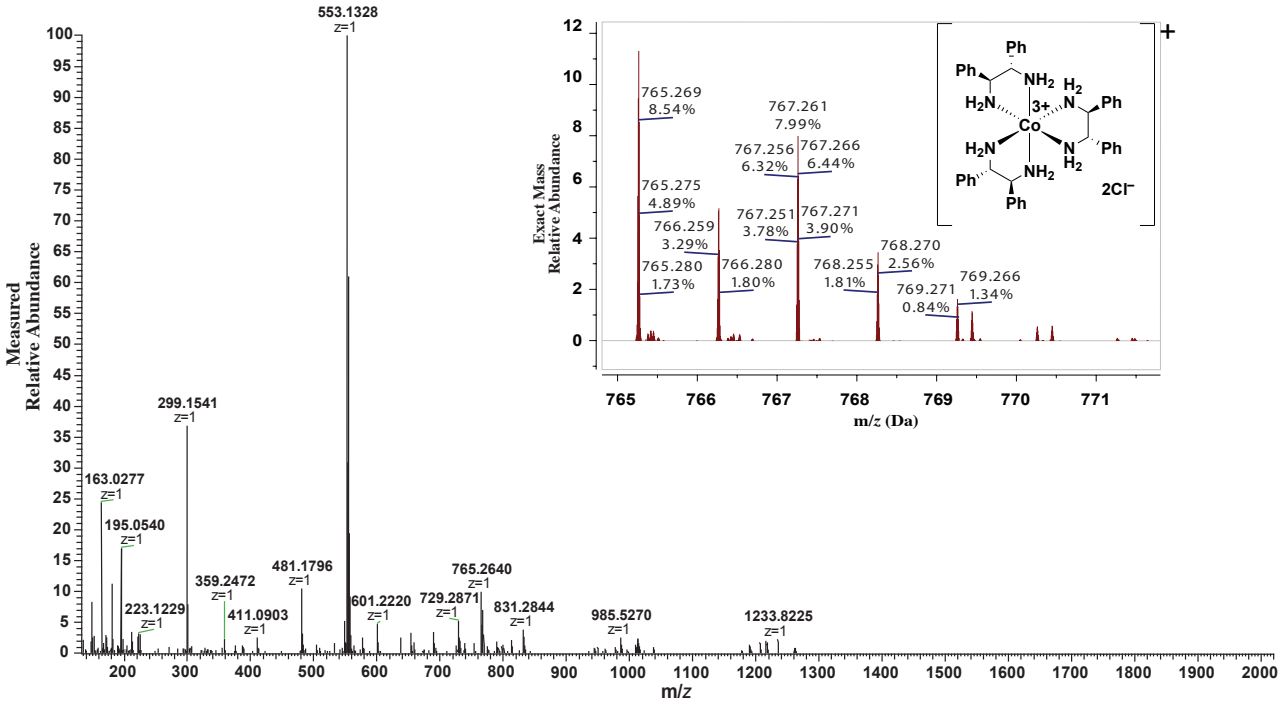

Cation	Observed $[M]^+$ (Calculated $[M]^+$)	*z*	I (%)	Comment
$[Co(dpen)_2]^{3+}$ $2Cl^-$	553.13 (553.13)	+1	100	**Most Intense**
$[Co(dpen)_2]^{3+}$ Cl^-OAc^-	577.18 (577.18)	+1	2.63	
$[Co(dpen)_2]^{3+}$ $2OAc^-$	601.22 (601.22)	+1	4.92	
$[Co(dpen)_3]^{3+}$ $2Cl^-$	765.26 (765.26)	+1	11.31	
$[Co(dpen)_3]^{3+}$ Cl^-OAc^-	789.31 (789.31)	+1	2.06	
$[Co(dpen)_3]^{3+}$ $2OAc^-$	813.35 (813.35)	+1	1.80	
Unknown	1568.56	+1	0.06	**Greatest m/z**

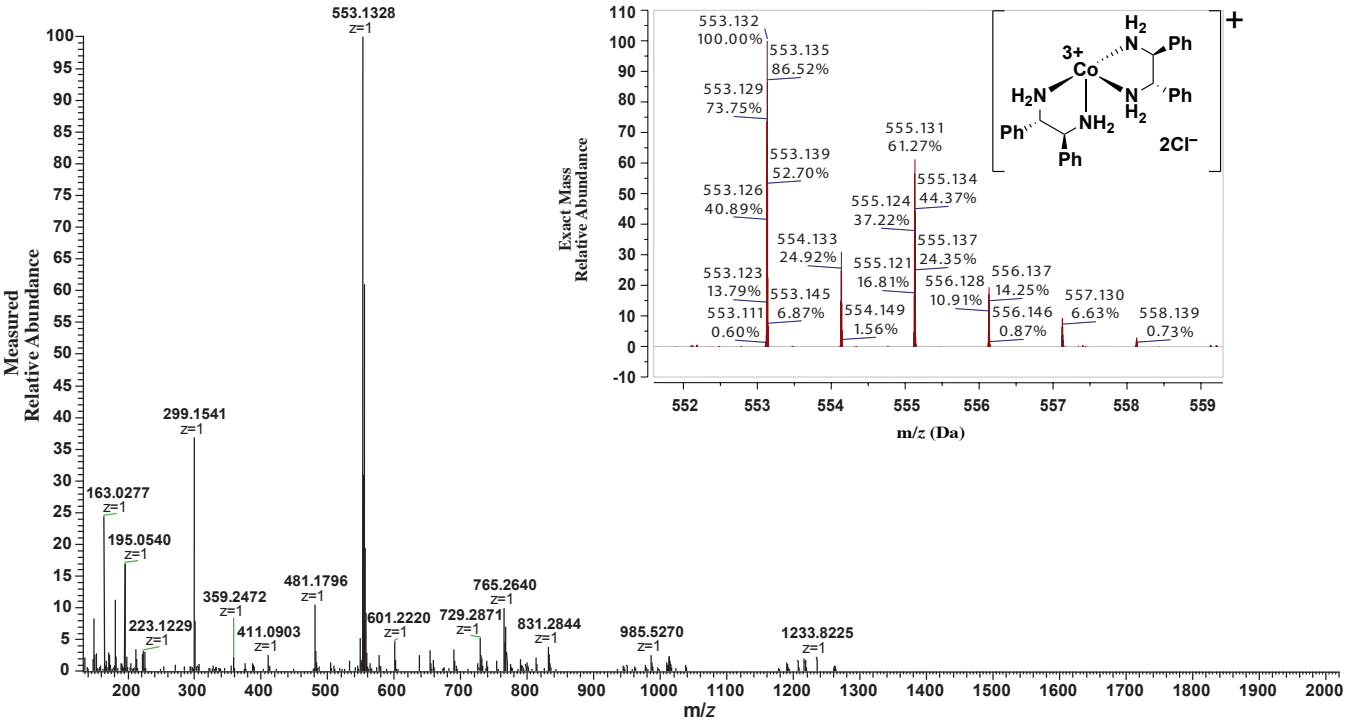
Measured
Relative Abundance
m/z
553.1328
z=1
299.1541
z=1
163.0277
z=1
195.0540
z=1
359.2472
z=1
481.1796
z=1
223.1229
z=1
411.0903
z=1
601.2220
z=1
729.2871
z=1
765.2640
z=1
831.2844
z=1
985.5270
z=1
1233.8225
z=1
Exact Mass
Relative Abundance
m/z (Da)
553.132
100.00%
553.135
86.52%
553.129
73.75%
553.139
52.70%
553.126
40.89%
555.131
61.27%
555.134
44.37%
555.124
37.22%
554.133
24.92%
555.137
24.35%
553.123
13.79%
555.121
16.81%
556.137
14.25%
553.145
6.87%
556.128
10.91%
553.111
0.60%
554.149
1.56%
556.146
0.87%
557.130
6.63%
558.139
0.73%
3+
Co
H2N
NH2
N
H2
Ph
Ph
Ph
Ph
2Cl−
+

Sample 2: Λ-(*S*,*S*)-$[Co(dpen)_3]^{3+}$ $3Cl^-$ • $3H_2O$*

Other Species Used in Synthesis: $Co(OAc)_2$; MeOH

*Purified on Dowex column

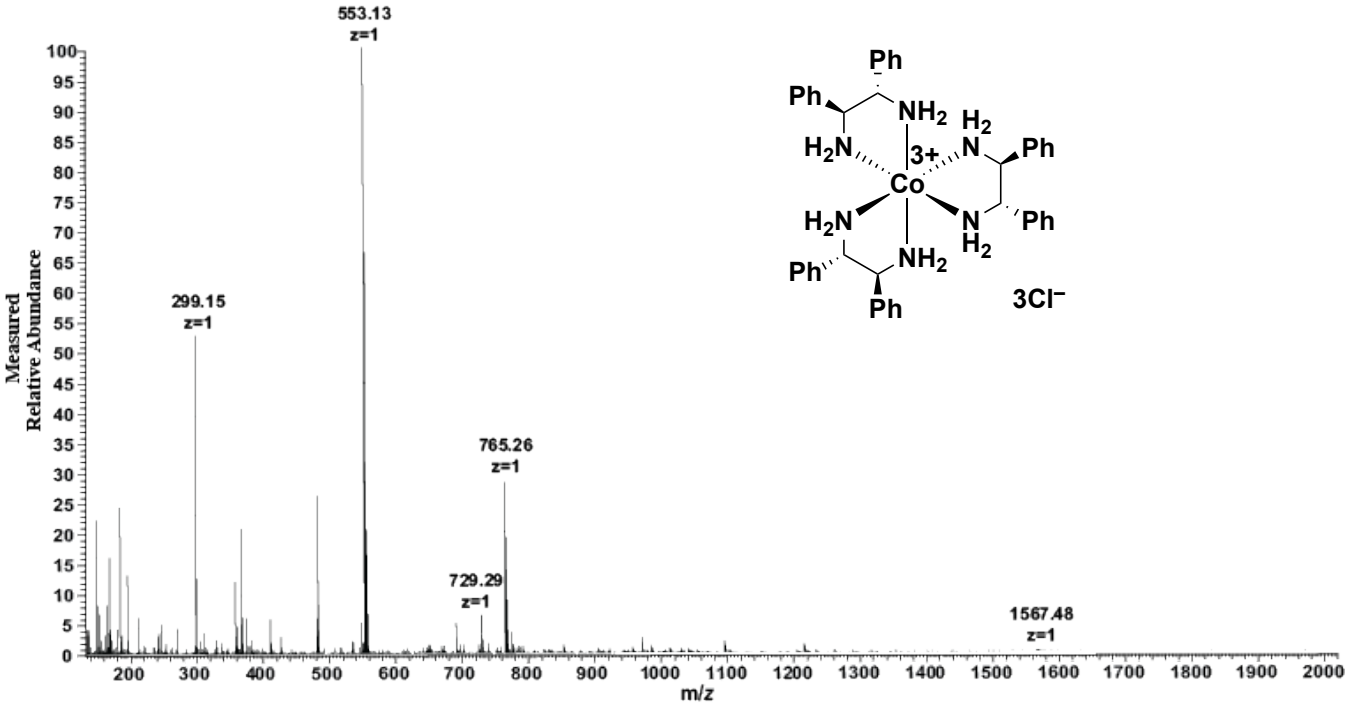

Cation	Observed $[M]^+$ (Calculated $[M]^+$)	z	I (%)	Comment
$[Co(dpen)_2]^{3+}$ $2Cl^-$	553.13 (553.13)	+1	100	**Most Intense**
$[Co(dpen)_3]^{3+}$ Cl^- $(-H^+)$	729.29 (729.29)	+1	5.67	Loss of H^+
$[Co(dpen)_3]^{3+}$ $2Cl^-$	765.26 (765.26)	+1	28.20	
Unknown	1567.48	+1	0.21	**Greatest m/z**

Sample 3: Λ-(*S*,*S*)-$[Co(dpen)_3]^{3+}$ $2Cl^-BAr_f^-$ • $2H_2O$

Other Species Used in Synthesis: $Co(OAc)_2$; MeOH; DCM

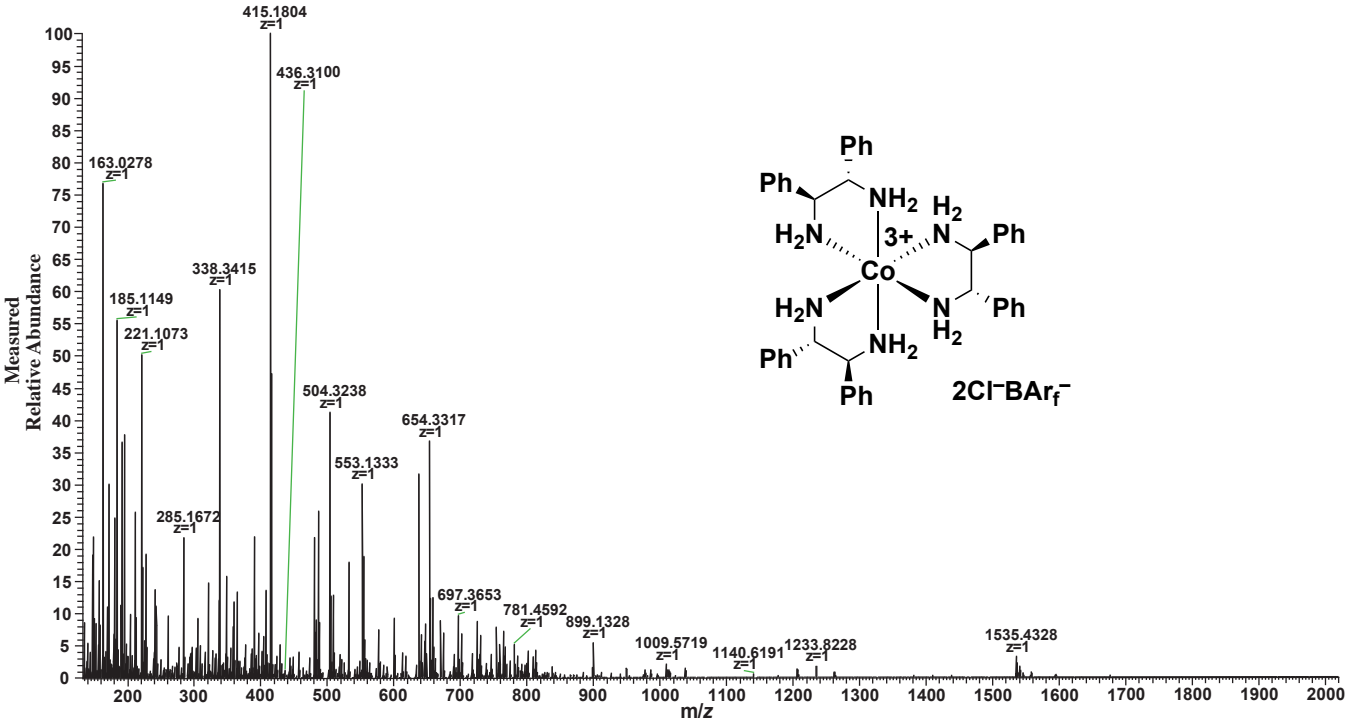

Cation	Observed $[M]^+$ (Calculated $[M]^+$)	*z*	I (%)	Comment
$[Co(en)_3]^{3+}$ $3OAc^-$ ($-H^+$)	415.18 (416.18)	+1	100	**Most Intense**; loss of H^+
$[Co(dpen)_2]^{3+}$ $2Cl^-$	553.13 (553.13)	+1	29.82	
$[Co(dpen)_2]^{3+}$ Cl^-OAc^-	577.18 (577.18)	+1	7.47	
$[Co(dpen)_2]^{3+}$ $2OAc^-$	601.22 (601.22)	+1	9.48	
$[Co(dpen)_3]^{3+}$ $2Cl^-$	765.27 (765.26)	+1	7.24	
$[Co(dpen)_3]^{3+}$ Cl^-OAc^-	789.31 (789.31)	+1	1.19	
$[Co(dpen)_3]^{3+}$ $2OAc^-$	813.36 (813.35)	+1	3.57	
$[Co(dpen)_3]^{3+}$ $Cl^-BAr_f^-$	1593.36 (1593.36)	+1	0.45	**Greatest m/z**

Sample 4: Λ-(*S*,*S*)-$[Co(dpen)_3]^{3+}$ $2Cl^-BAr_f^-$ • $2H_2O$*

Other Species Used in Synthesis: $Co(OAc)_2$; MeOH; DCM

*Synthesized from Λ-(*S*,*S*)-$[Co(dpen)_3]^{3+}$ $3Cl^-$ • $3H_2O$* purified on Dowex

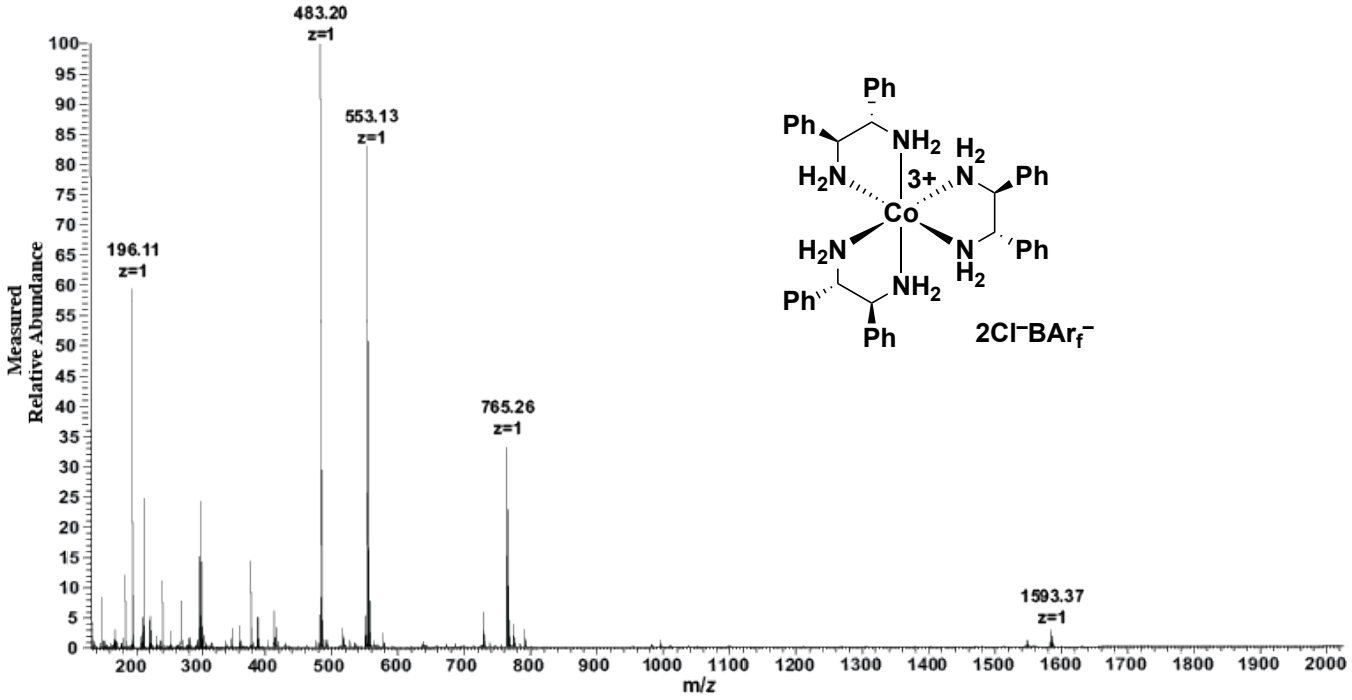

Cation	Observed $[M]^+$ (Calculated $[M]^+$)	z	I (%)	Comment
Unknown	483.20	+1	100	**Most Intense**
$[Co(dpen)_2]^{3+}$ $2Cl^-$	553.13 (553.13)	+1	83.13	
$[Co(dpen)_2]^{3+}$ Cl^-OAc^-	577.18 (577.18)	+1	2.42	
$[Co(dpen)_3]^{3+}$ Cl^- $(-H^+)$	729.29 (729.29)	+1	5.80	Loss of H^+
$[Co(dpen)_3]^{3+}$ $2Cl^-$	765.26 (765.26)	+1	33.15	
$[Co(dpen)_3]^{3+}$ BAr_f^- $(-H^+)$	1557.37 (1557.38)	+1	0.91	Loss of H^+
$[Co(dpen)_3]^{3+}$ $Cl^-BAr_f^-$	1593.37 (1593.36)	+1	2.80	**Greatest m/z**

Sample 5: Δ-(*S*,*S*)-$[Co(dpen)_3]^{3+}$ $2Cl^-BAr_f^-$ • H_2O

Other Species Used in Synthesis: $Co(OAc)_2$; MeOH; DCM

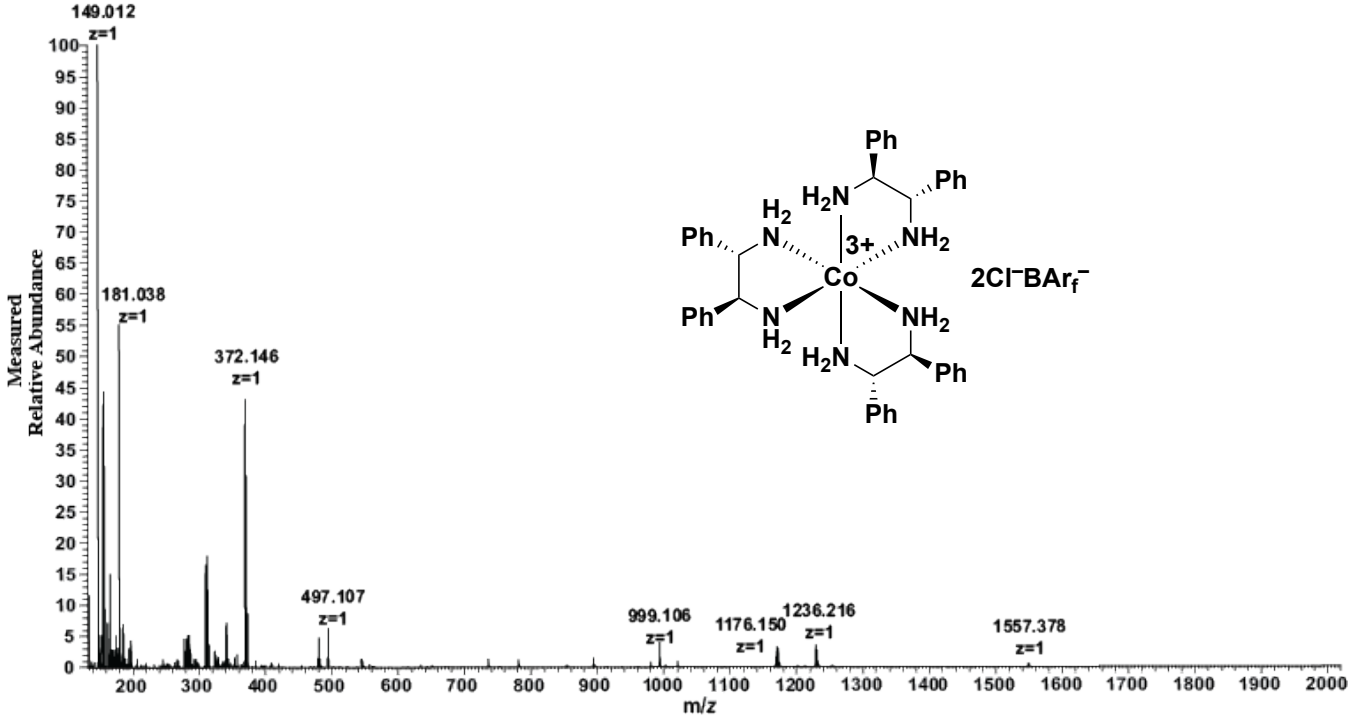

Cation	Observed $[M]^+$ (Calculated $[M]^+$)	*z*	I (%)	Comment
Unknown	149.01	+1	100	**Most Intense**
$[Co(dpen)_3]^{3+}$	231.77 (231.78)	+3	0.07	
$[Co(dpen)_3]^{3+}$ BAr_f^- $(-H^+)$	1557.38 (1557.38)	+1	0.60	**Greatest m/z; loss of H^+**

Sample 6: Λ-(*S*,*S*)-$[Co(dpen)_3]^{3+}$ $3BF_4^-$ • $2H_2O$

Other Species Used in Synthesis: $Co(OAc)_2$; MeOH

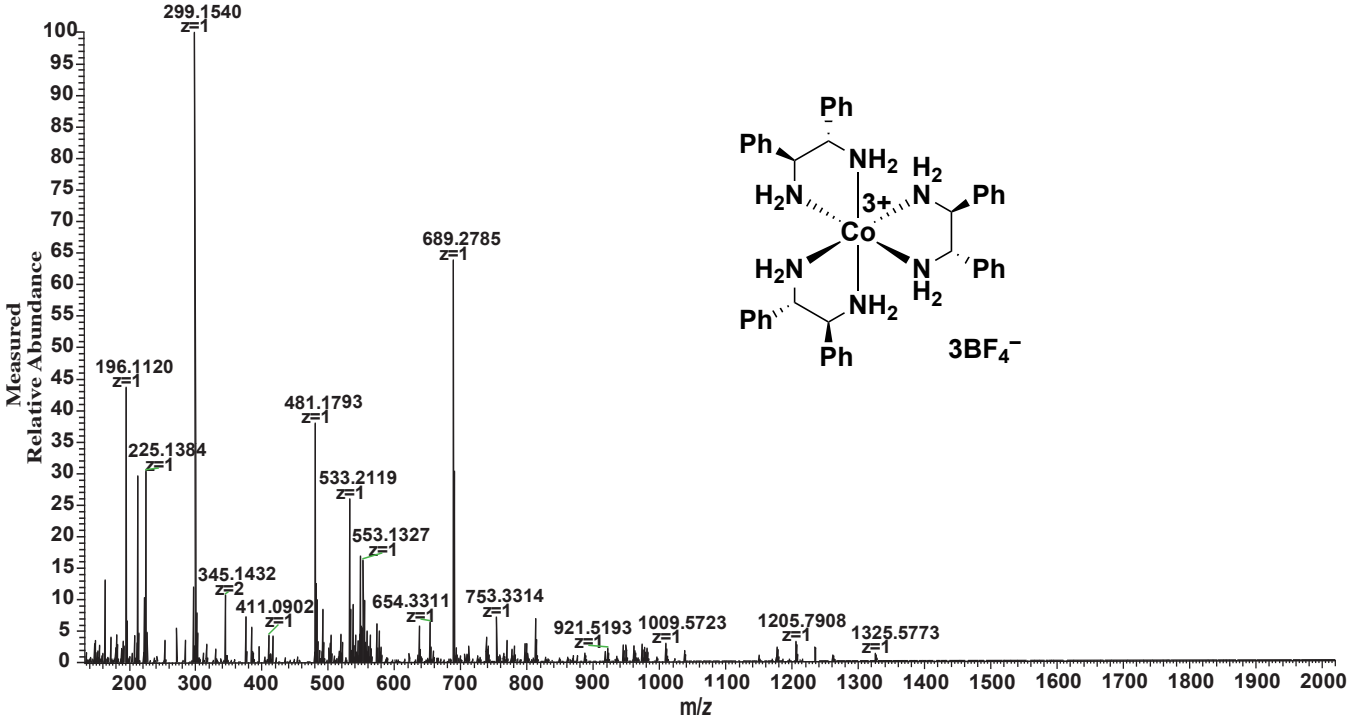

Cation	Observed $[M]^+$ (Calculated $[M]^+$)	*z*	I (%)	Comment
Unknown	299.15	+1	100	**Most Intense**
$[Co(dpen)_2]^{3+}$ $2Cl^-$	553.13 (553.13)	+1	15.98	
$[Co(dpen)_2]^{3+}$ Cl^-OAc^-	577.18 (577.18)	+1	4.91	
$[Co(dpen)_3]^{3+}$ BF_4^- $(-H^+)$	781.32 (781.32)	+1	2.50	Loss of H^+
$[Co(dpen)_3]^{3+}$ $2OAc^-$	813.35 (813.35)	+1	6.74	
$[Co(dpen)_3]^{3+}$ $2BF_4^-$	869.33 (869.33)	+1	0.96	
Unknown	1325.88	+1	1.18	**Greatest m/z**

Sample 7: Λ-(*S*,*S*)-$[Co(dpen)_3]^{3+}$ $3PF_6^-$ • $6H_2O$

Other Species Used in Synthesis: $Co(OAc)_2$; MeOH

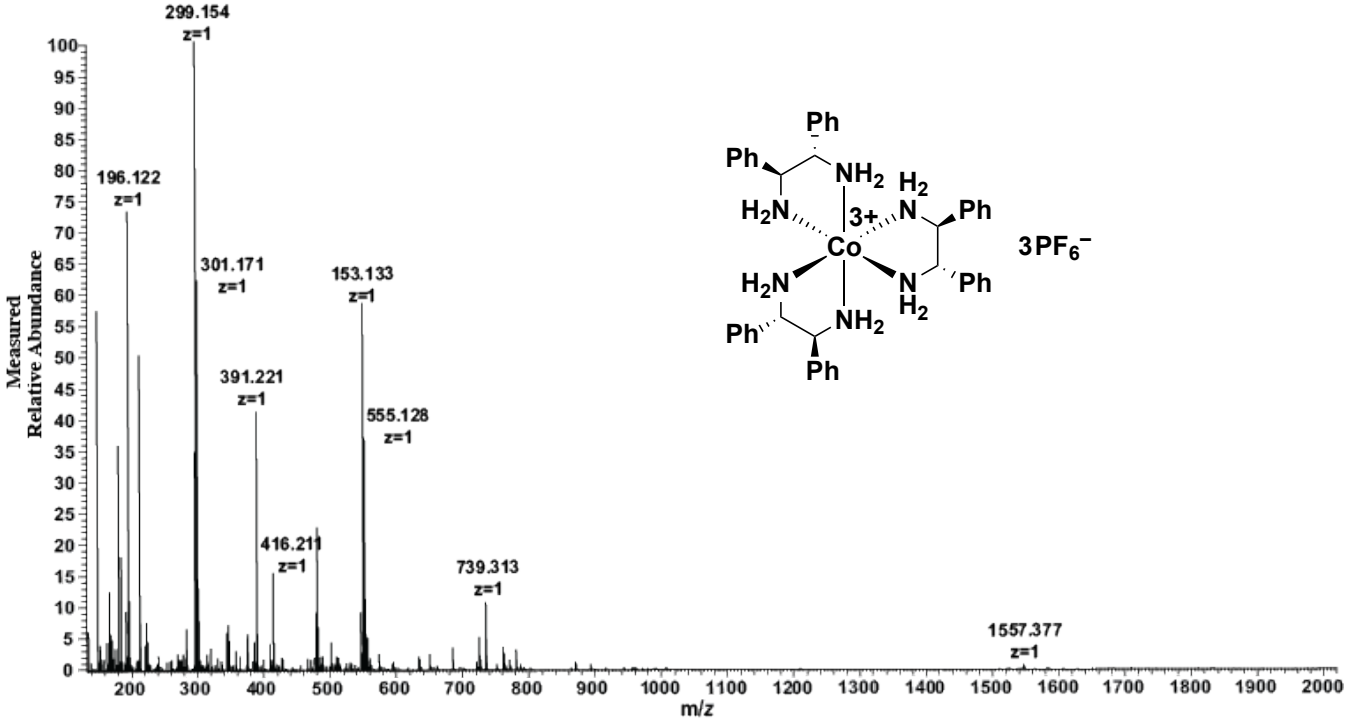

Cation	Observed $[M]^+$ (Calculated $[M]^+$)	*z*	I (%)	Comment
Unknown	299.15	+1	100	**Most Intense**
$[Co(dpen)_2]^{3+}$ $2Cl^-$	553.13 (553.13)	+1	58.37	
$[Co(dpen)_2]^{3+}$ Cl^-OAc^-	577.18 (577.18)	+1	2.73	
$[Co(dpen)_3]^{3+}$ $2Cl^-$	765.27 (765.26)	+1	3.81	
$[Co(dpen)_3]^{3+}$ $Cl^-BAr_f^-$	1593.36 (1593.36)	+1	0.13	**Greatest m/z**

Sample 8: Λ-(*S*,*S*)-$[Co(dpen)_3]^{3+}$ $Cl^-BAr_f^-Nic^-$ • $2H_2O$

Other Species Used in Synthesis: $Co(OAc)_2$; MeOH; DCM

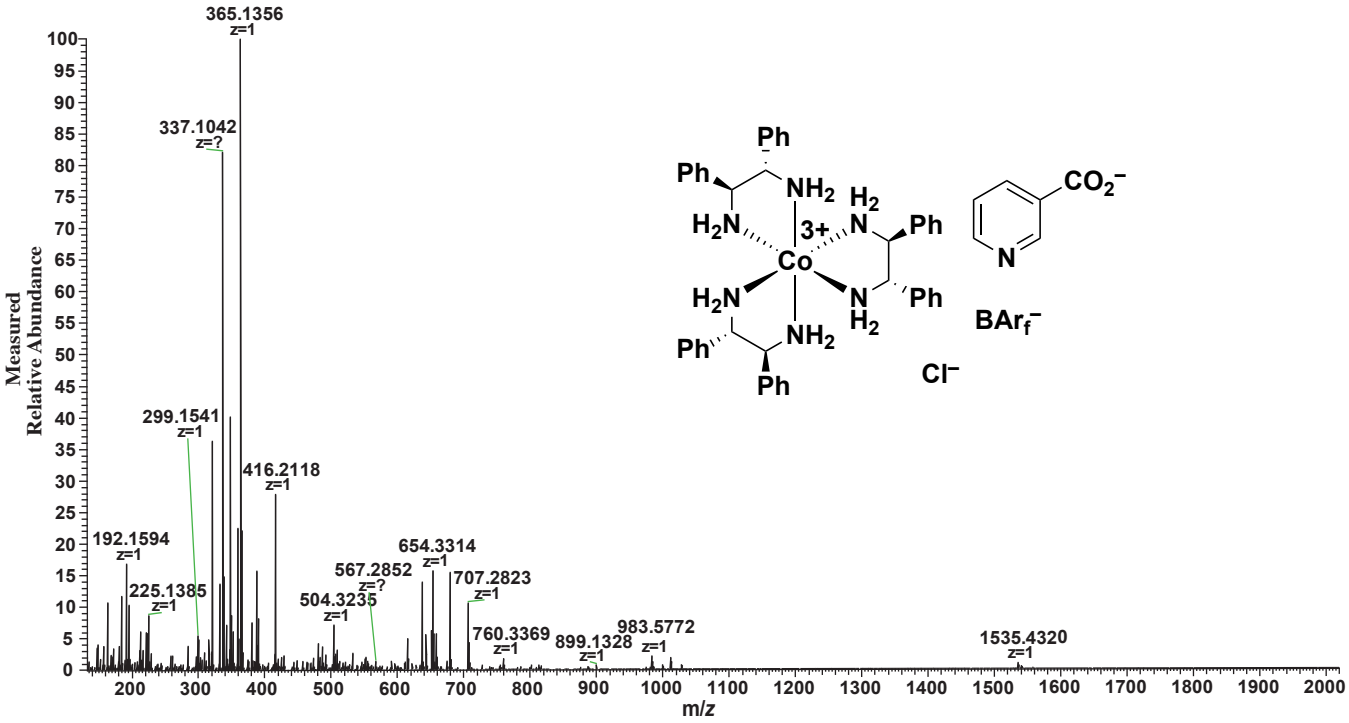

Cation	Observed $[M]^+$ (Calculated $[M]^+$)	*z*	I (%)	Comment
Unknown	365.14	+1	100	**Most Intense**
$[Co(dpen)_3]^{3+}$ Nic^- ($-H^+$)	816.35 (816.34)	+1	0.54	Loss of H^+
$[Co(dpen)_3]^{3+}$ BAr_f^- ($-H^+$)	1557.42 (1557.38)	+1	0.33	Loss of H^+
Unknown	1646.39	+1	0.02	**Greatest m/z**

Sample 9: Λ-(*S*,*S*)-$[Co(dpen)_3]^{3+}$ $3SbF_6^-$ • $5H_2O$

Other Species Used in Synthesis: $Co(OAc)_2$; MeOH

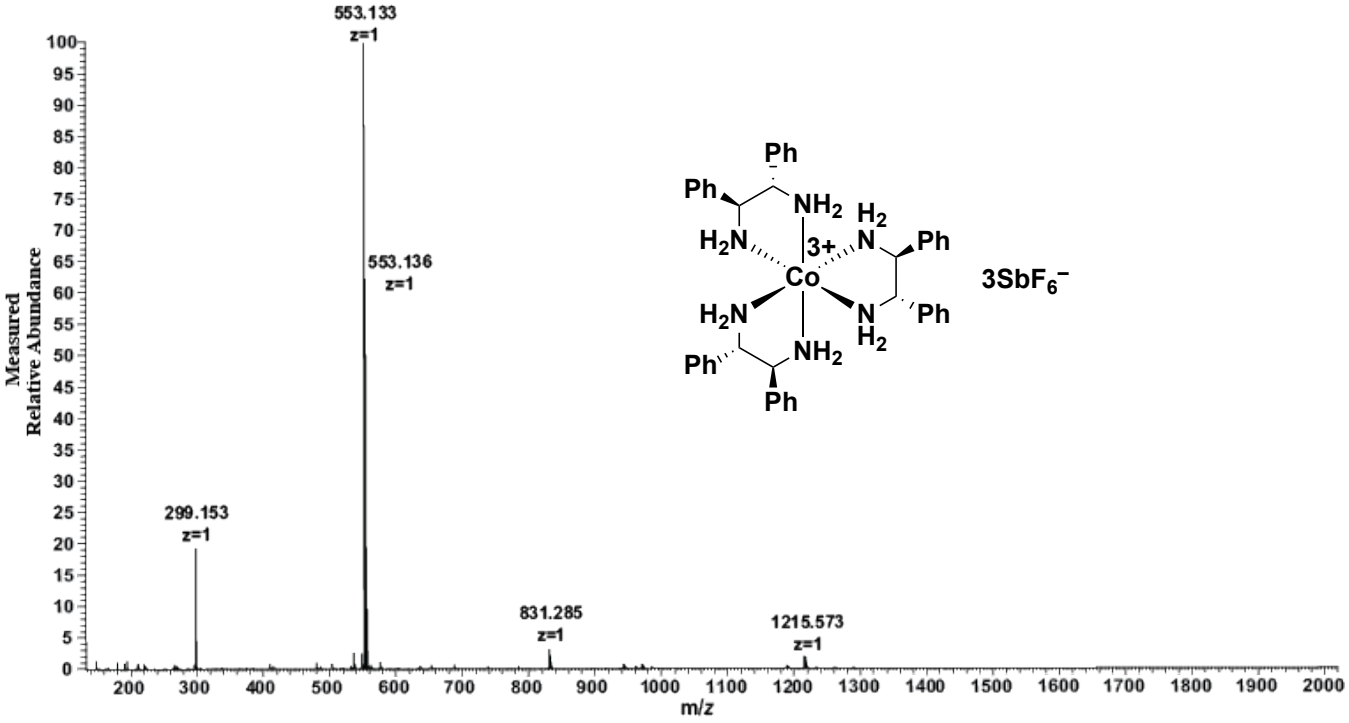

Cation	Observed $[M]^+$ (Calculated $[M]^+$)		I (%)	Comment
Unknown	299.15	+1	19.38	
$[Co(dpen)_2]^{3+}$ $2Cl^-$	553.13	+1	100	**Most Intense**
Unknown	1344.57	+1	0.10	**Greatest m/z**

Sample 10: Λ-(*S*,*S*)-$[Co(dpen)_3]^{3+}$ 3(1R)-camphorSO_3^- • $2H_2O$

Other Species Used in Synthesis: $Co(OAc)_2$; MeOH; DCM

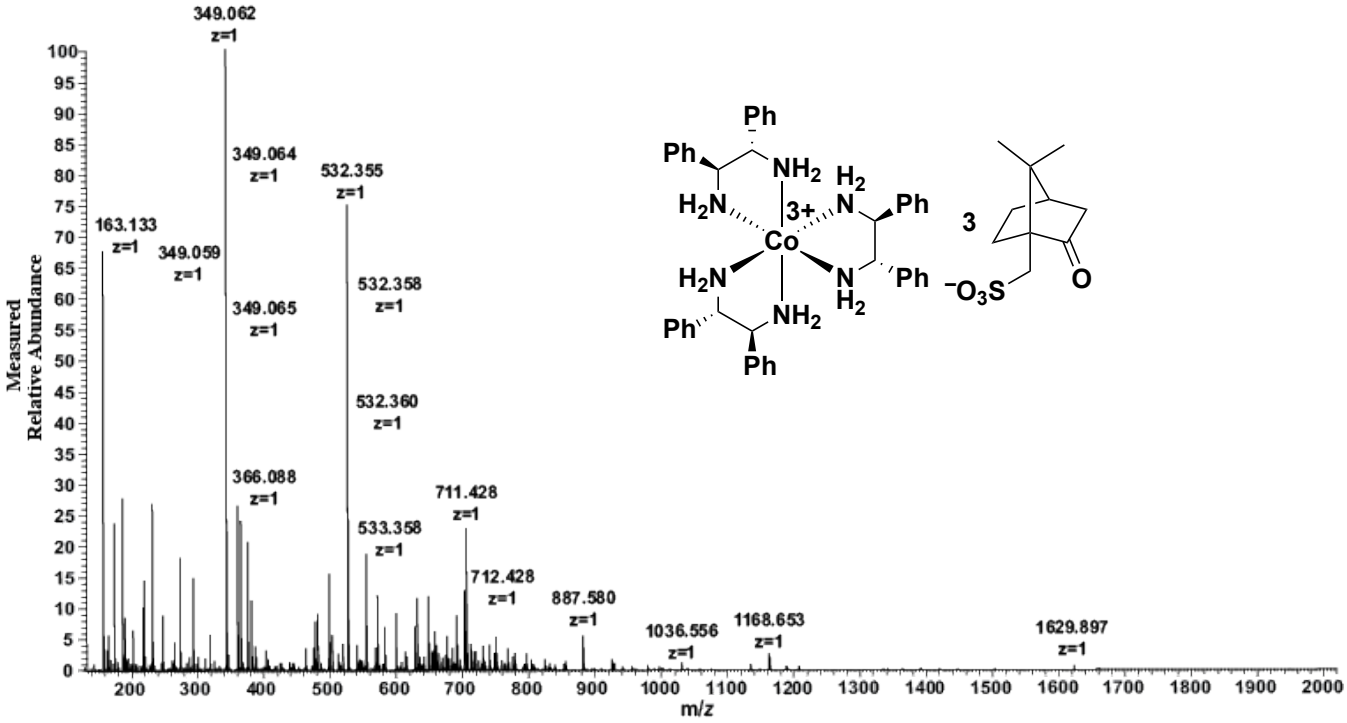

Cation	Observed $[M]^+$ (Calculated $[M]^+$)	*z*	I (%)	Comment
Unknown	349.06	+1	100	**Most Intense**
Unknown	1666.90	+1	0.28	**Greatest m/z**

Sample 11: Λ-(*S*,*S*)-[Co(dpen)$_3$]$^{3+}$ 3(S)-BINOLPA$^-$ • 4H$_2$O

Other Species Used in Synthesis: Co(OAc)$_2$; MeOH; DCM; NaOH

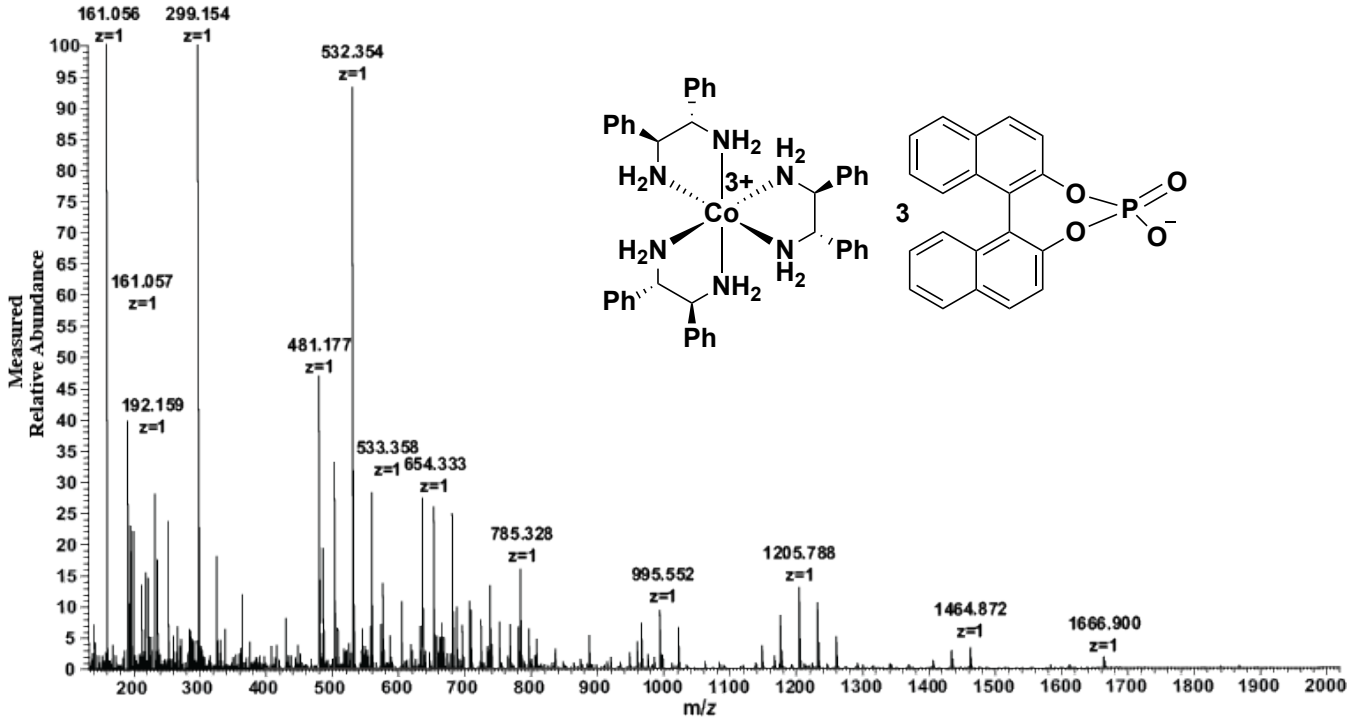

Cation	Observed [M]$^+$ (Calculated [M]$^+$)	*z*	I (%)	Comment
Unknown	161.06	+1	100	**Most Intense**
Unknown	1666.90	+1	1.71	**Greatest m/z**

Sample 12: Λ-(*S*,*S*)-$[Pt(en)_3]^{4+}$ $4BAr_f^-$ • $17H_2O$

Other Species Used in Synthesis: $Co(OAc)_2$; MeOH; DCM

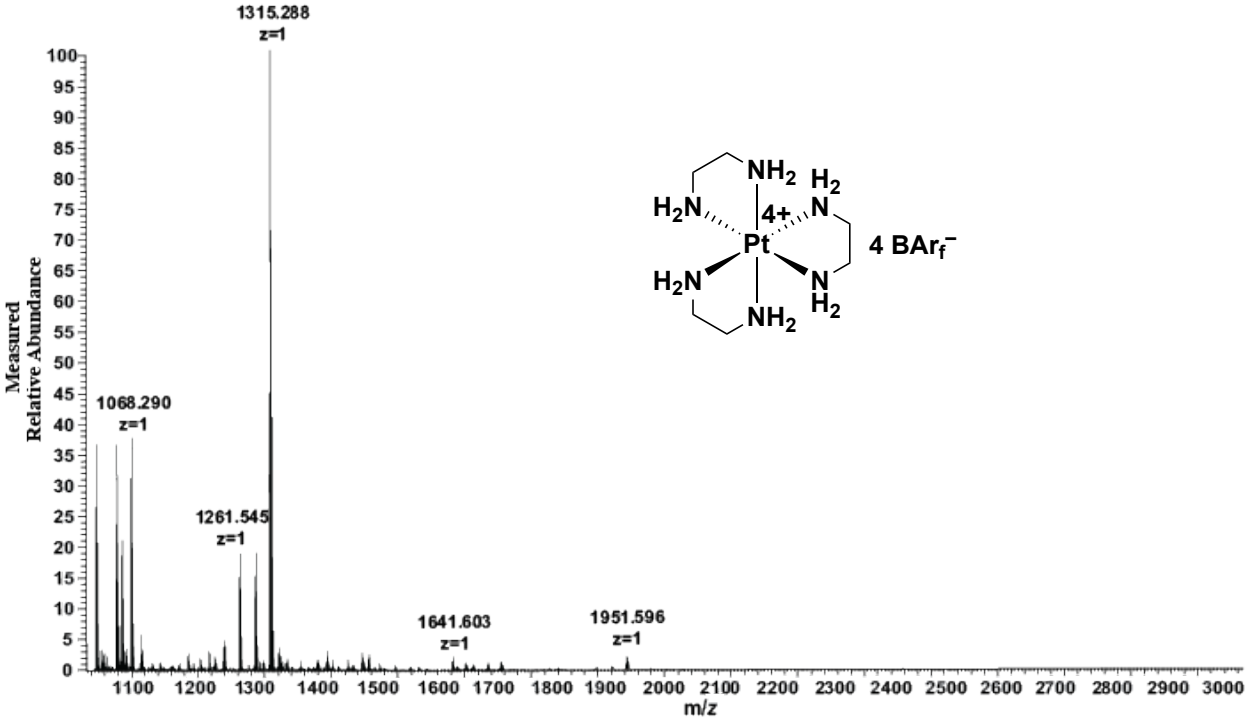

Cation	Observed $[M]^+$ (Calculated $[M]^+$)	*z*	I (%)	Comment
Unknown	1315.29	+1	100	**Most Intense**
Unknown	2445.71	+1	0.19	**Greatest m/z**